Current Research in Toxicology 3 (2022) 100071

Contents lists available at ScienceDirect

Current Research in Toxicology

journal homepage: www.elsevier.com/locate/crtox

Assessment of the effects of organic vs. inorganic arsenic and mercury in *Caenorhabditis elegans*

Jessica Camacho [a], Aline de Conti [b], Igor P. Pogribny [b], Robert L. Sprando [a], Piper Reid Hunt [a,*]

[a] Food and Drug Administration, Center for Food Safety and Applied Nutrition, Office of Applied Research and Safety Assessment, 8301 Muirkirk Road, Laurel, MD 20708, United States
[b] Food and Drug Administration, National Center for Toxicological Research, 3900 NCTR Rd, Jefferson, AR 72079, United States

ARTICLE INFO

Handling Editor Thomas B Knudsen

Keywords:
Alternative Toxicity Model
Arsenic
Inorganic
Mercury
Organic
Predictive Toxicology

ABSTRACT

Exposures to mercury and arsenic are known to pose significant threats to human health. Effects specific to organic vs. inorganic forms of these toxic elements are less understood however, especially for organic dimethylarsinic acid (DMA), which has recently been detected in pups of rodent dams orally exposed to inorganic sodium (meta)arsenite (NaAsO2). *Caenorhabditis elegans* is a small animal alternative toxicity model. To fill data gaps on the effects of DMA relative to NaAsO2, *C. elegans* were exposed to these two compounds alongside more thoroughly researched inorganic mercury chloride (HgCl2) and organic methylmercury chloride (meHgCl). For timing of developmental milestone acquisition in *C. elegans*, meHgCl was 2 to 4-fold more toxic than HgCl2, and NaAsO2 was 20-fold more toxic than DMA, ranking the four compounds meHgCl > HgCl2 > NaAsO2 ≫ DMA for developmental toxicity. Methylmercury induced significant decreases in population locomotor activity levels in developing *C. elegans*. DMA was also associated with developmental hypoactivity, but at >100-fold higher concentrations than meHgCl. Transcriptional alterations in native genes were observed in wild type *C. elegans* adults exposed to concentrations equitoxic for developmental delay in juveniles. Both forms of arsenic induced genes involved in immune defense and oxidative stress response, while the two mercury species induced proportionally more genes involved in transcriptional regulation. A transgenic bioreporter for activation of conserved proteosome specific unfolded protein response was strongly activated by NaAsO2, but not DMA at tested concentrations. HgCl2 and meHgCl had opposite effects on a bioreporter for unfolded protein response in the endoplasmic reticulum. Presented experiments indicating low toxicity for DMA in *C. elegans* are consistent with human epidemiologic data correlating higher arsenic methylation capacity with resistance to arsenic toxicity. This work contributes to the understanding of the accuracy and fit-for-use categories for *C. elegans* toxicity screening and its usefulness to prioritize compounds of concern for further testing.

1. Introduction

The Agency for Toxic Substances and Disease Registry (ATSDR) prioritizes chemical compounds of concern based on their toxicity and potential for human exposure. Arsenic and mercury are at or near the top of this list of hazardous substances and are known to be especially harmful during early development (ATSDR, 2019; Congress, 2021; FDA, 2020). The bioavailability and effects of arsenic and mercury are known to vary based on chemical form to the extent that safety and mode of action assessments for one form do not apply to other forms, highlighting the need to better understand their relative toxicities (Davidson et al., 2004; Luvonga et al., 2020). The Food and Drug Administration's (FDA's) "Closer to Zero" initiative identifies actions the agency will take towards reducing exposure to toxic elements from foods consumed by babies and young children and supports continuing research on the impacts of toxic elements during development (FDA, 2021). For mercury, lower limits on intake levels are recommended for methylmercury relative to mercury chloride

Abbreviations: DMA, dimethylarsinic acid; DEGs, Differentially Expressed Genes; ER, endoplasmic reticulum; EXT, extinction (a measure of optical density); GO, gene ontology; HgCl2, mercury(ii) chloride; iAs, inorganic arsenic; L1, first larval stage *C. elegans*; LD50, the median lethal dose per kilogram of body weight; LOEL, lowest observed effect level; meHgCl, methylmercury chloride; NaAsO2, sodium (meta)arsenite; NOEL, no observed effect level; OxStrR, Oxidative Stress Response; TOF, time of flight (a measure of size); UPR, Unfolded Protein Response.

* Corresponding author.
E-mail address: Piper.Hunt@fda.hhs.gov (P.R. Hunt).

https://doi.org/10.1016/j.crtox.2022.100071
Received 21 November 2021; Revised 26 March 2022; Accepted 20 April 2022

due to the neurodevelopmental toxicity of organic mercury (ATSDR, 1999; EFSA, 2012). For inorganic arsenic (iAs), the provisional tolerable weekly intake (PTWI) established by the World Health Organization in 1986 of 15 μg/kg body weight was withdrawn in 2009 due to carcinogenic effects at lower exposures, and a new PTWI has not been set (Naess et al., 2020). Recently, dimethylarsinic acid (DMA) was found in the pups of rodent dams fed iAs (Twaddle et al., 2018), raising concerns about the developmental effects of DMA. iAs is generally considered more toxic than organic forms of arsenic, however mammalian oral toxicity data for organic arsenic species is limited, particularly for DMA (EFSA, 2009; FAOUN/WHO, 2011; FDA, 2016). DMA has been detected in rice, and since rice flour is an ingredient in many baby foods (FDA, 2016), more information on the developmental effects of DMA is needed.

The FDA's Predictive Toxicology Roadmap supports the identification, development, and assessment of emerging methods and new technologies for use in risk assessments for regulatory purposes (FDA, 2017). The qualification and progress towards utilization of these leading-edge predictive toxicology tools are priorities for FDA's Center for Food Safety and Applied Nutrition (CFSAN, 2015). *Caenorhabditis elegans* is a small, non-pathogenic nematode that can be maintained at low cost and handled using standard *in vitro* equipment and techniques, and its 3-day development from egg to egg-laying adult allows for rapid developmental toxicity testing. *C. elegans* assays provide data from a whole animal with intact and metabolically active digestive, reproductive, sensory, and neuromuscular systems (Hunt et al., 2020). There is significant conservation between *C. elegans* and humans for biological pathways involved in organismal development and neurotransmission (Leung et al., 2008; Ruszkiewicz et al., 2018), and the toxicodynamics for many types of chemicals is similar in *C. elegans* and mammals (Hartman et al., 2021). Conserved alimentary features such as acidic and non-acidic portions of the digestive tract, digestive enzymes, and brush boarder function make *C. elegans* a potential model for predictive oral toxicity assessment (Hunt, 2017). A single *C. elegans* technician can assess a dozen or more compounds or concentrations in a week for endpoints such as viability, locomotor activity, developmental timing, or pathway of toxicity specific transgene expression. While this type of low-to-medium-throughput *C. elegans* screening cannot replace a descriptive toxicology study in lab mammals, it is very rapid and inexpensive by comparison, and can provide useful information on conserved modes of toxic action and apical endpoint responses (Avila et al., 2020; Hartman et al., 2021; Masjosthusmann et al., 2018; Parish et al., 2020). Several studies have demonstrated that toxicity ranking screens in *C. elegans* can predict developmental toxicity or LD50 ranking in mammals (Boyd et al., 2010; Boyd et al., 2016; Hunt et al., 2012; Li et al., 2013), indicating that *C. elegans* has the potential to provide a bridge between *in vitro* human cell based assays and mammalian *in vivo* oral toxicity testing (Lagido et al., 2015).

Several lines of evidence indicate that *C. elegans* is a good model to study conserved aspects of toxic responses to arsenic. From worms to mammalian cell cultures, exposure to iAs activates the p38 mitogen-activated protein kinase cascade (Inoue et al., 2005; Kang and Lee, 2008; Wang et al., 2013), induces Nrf/SKN-1 regulated phase II detoxification enzymes and protein folding-sensitive molecular chaperones (Del Razo et al., 2001; Oliveira et al., 2009; Tam and Wang, 2020; Yu et al., 2016), alters innate immune function (Dangleben et al., 2013; Escudero-Lourdes, 2016; Ma et al., 2021), and has similar effects on mitochondrial function (Luz et al., 2016; Luz et al., 2017; Tam and Wang, 2020). The *C. elegans* model reflects some of the differing mammalian effects of organic vs. inorganic mercury. For rodents and *C. elegans*, meHgCl is more toxic than HgCl2 during early development, and has greater effects on locomotor activity (McElwee and Freedman, 2011; Wyatt et al., 2016). For mammals and *C. elegans*, methylmercury is a developmental neurotoxin, and the very young are more sensitive than adults to its effects (Helmcke et al., 2009; Ruszkiewicz et al., 2018). Effects of organic vs. iAs may also be conserved. Therefore, we assessed the effects of DMA, sodium (meta)arsenite (NaAsO2), methylmercury chloride (meHgCl), and mercury chloride (HgCl2) on *C. elegans* development and stage specific locomotor activity, adult native gene expression, and pathway of toxicity specific transgene expression.

2. Material and methods

2.1. Chemicals

Test chemicals (Table 1) were purchased from MilliporeSigma (Burlington, MA). Fresh dosing solutions were prepared for each experiment in Milli-Q purified water within two hours prior to dosing. Test chemicals readily dissolved in water with exception of meHgCl, which was first dissolved in water at 200 μg/ml for 30 min with stirring prior to dilution and dosing.

2.2. Worm maintenance

C. elegans wild type N2, LD1171 (ldIs3 [*gcs-1*p::GFP + rol-6(su1006)]), CL2166 (dvIs19 [(pAF15)*gst-4*p::GFP::NLS] III), SJ4005 (zcIs4 [*hsp-4*p::GFP] V), and SJ4003 (zcIs3 [*aip-1*p::GFP] I) strains were obtained from the *Caenorhabditis* Genetics Center (CGC), which is funded by the NIH Office of Research Infrastructure Programs (P40 OD010440). Strains were grown under continuously well-fed conditions on agar plates with OP50 *E. coli* as a feeder organism for three generations prior to hypochlorite treatment to isolate eggs and transfer to *C. elegans* Habitation Medium (CeHM) as previously described (Nass and Hamza, 2007). Growth in CeHM containing 20% non-fat cows' milk allows *C. elegans* larvae to develop at the same rate as with *E. coli* (Clegg et al., 2002; Sprando et al., 2009). Aliquots were frozen at −80 °C soon after transfer to CeHM, and fresh aliquots were thawed every 6 months to avoid genetic drift in test cohorts. Cultures were fed fresh CeHM regularly in a biological cabinet using sterile technique and maintained at 20 °C on shakers in hot/cold incubators in vented, polystyrene flasks. Thawed aliquots were allowed a minimum of three weeks growth in CeHM prior to toxicity testing to minimize effects of freeze-thawing on stress resistance and gene expression. For test cohorts, well-fed gravid *C. elegans* were subjected to hypochlorite treatment to isolate eggs. Eggs were allowed to hatch overnight in non-nutrient M9 buffer for 19 +/- 1 hr to obtain age-synchronized first larval stage (L1) worms. Isolates containing > 1 dauer per approximately 5,000 eggs were discarded along with the culture flasks they were obtained from to ensure cohorts originated from well-fed cultures and were exposed to minimal amounts of dauer pheromone. Synchronized L1s were centrifuged, resuspended to approximately 900 worms per mL CeHM, and then either dosed immediately for developmental toxicity assessment, or maintained with regular media changes for dosing at later stages.

2.3. Developmental toxicity testing

3-day exposures of synchronized L1s were conducted in sterile CELLSTAR 12-well polystyrene plates with lids and carried out in two wMicroTrackers (InVivo Biosystems, Eugene, OR) side-by-side inside a 20 °C incubator. 100 μL of water or 10x dosing solution in water were added to 900 μL of L1s in CeHM in a diagonal pattern, with one water control and three dosed conditions per plate, and three replicate wells per condition. Each worm Development and Activity Test (wDAT) trial was performed as four independent experiments using freshly prepared L1 cohorts and dosing solutions. Over the four experiments, each well placement was used once and only once for each condition to account for small differences in wMicroTracker (wMT) infrared beam placement. wMT output was read in 30 min

Table 1
Chemicals Selected for Testing.

Compound *	Abbreviation	CAS RN	LD50	Oral RfD	TWI
sodium (meta)arsenite	NaAsO2	7784–46-5	41 mg/kg (rat, oral)	0.3 μg/kg-day (IRIS, 1991)	withdrawn #
dimethylarsinic acid (DMA^V)	DMA	75–60-5	700 mg/kg (rat, oral) 1.2 g/kg (mouse, oral)	not established	not established
mercury chloride	HgCl2	7487–94-7	1 mg/kg (rat, oral) 6 mg/kg (mouse, oral)	0.3 μg/kg-day (IRIS, 1995)	4 μg Hg/kg-week (EFSA, 2012)
methylmercury chloride	meHgCl	115–09-3	30 mg/kg (rat, oral) 58 mg/kg (mouse, oral)	0.1 μg/kg-day (IRIS, 2001)	1.3 μg Hg/kg-week (EFSA, 2012)

CAS RN: The Chemical Abstracts Service (CAS) Registration Number (RN) is a unique numerical identifier designating a specific substance.
LD50: the median lethal dose per kilogram of body weight.
RfD: Reference Dose for chronic oral exposure, an estimate of a daily exposure that is likely to be without.
an appreciable risk of deleterious effects during a lifetime.
TWI: tolerable weekly intake, the amount per kilogram of body weight that can be ingested per week without risk of adverse health effects.
Provisional TWI of 15 μg As/kg was withdrawn in 2009 as too high for safety (Naess et al., 2020).
* Compounds and CAS RNs listed are those purchased and used in this study. Reference values (LD50, RfD, and TWI) may be for slightly different compounds, for example the available oral RfD is for methylmercury, CAS RN 22967–92-6.

increments as mean beam-interruptions per condition over the three replicate wells. Peaks were smoothed by taking the mean of seven half-hour timepoints, and the highest value at the third larval stage (L3) was recorded as peak height for population locomotor activity, and the corresponding time as time to reach L3. Values were normalized to in-plate controls and presented as relative time to peak (delay) and relative peak height (population locomotor activity). Students' T-test p-values of < 0.05 were considered statistically significant. Based on differences between controls (listed as 0 L-R in graphs) from simultaneously run plates over the study, changes of $> 4\%$ for developmental delay and $> 5\%$ for locomotor activity were considered biologically significant.

2.4. Adult gene expression – Dosing

Worms were age-synchronized at L1 as described (section 2.2) and maintained until the fourth larval stage (L4). Wildtype N2 *C. elegans* reach mid-L4 at about 50 h post-L1 hatching at 20 °C, but transgenic strains can differ from the wildtype in the time to reach L4 due to their genetic alterations. Therefore instead of dosing at a standard timepoint, developmental morphology was closely monitored as previously described (Seydoux et al., 1993) in order to dose at mid-L4. All exposures were carried out in sterile Falcon 24-well polystyrene plates with lids and maintained on shakers in a 20 °C incubator. After the exposure period, worms were washed twice with M9 nematode buffer, and then either resuspended in TRIzol Reagent (ThermoFisher Scientific, Waltham, MA) and frozen for subsequent microarray assessments, or directly run through a Complex Object Parametric Analyzer and Sorter (COPAS™, Union Biometrica, Holliston, MA) for transgene expression analysis. For microarray assessment, N2 *C. elegans* were exposed from mid-L4 to 8 μM 5-Fluoro-2′-deoxyuridine (FUdR, a contraceptive used to avoid confounding embryonic and larval gene expression), and 24 h later 900 μL of adults in CeHM plus FUdR were dosed with 100 μL of 10x dosing solutions and exposed for 24 h. For COPAS assessment, *C. elegans* were exposed without FUdR from mid-L4 for 24 h. For SJ4005 *hsp-4*p::GFP assessment, both heat shock and tunicamycin (30 μg/ml in 0.1% DMSO) were tested for use as positive controls (Hou et al., 2014; Tsialikas and Argon, 2017). Heat stress treatments of *C. elegans* in CeHM at 30 °C for 1, 3 and 5 h did not induce a change in GFP levels, while 30 μg/ml tunicamycin resulted in an average 1.7x increase in expression, so tunicamycin was utilized as the positive control (Supplemental Fig. 1A).

2.5. RNA extraction and gene expression analysis using microarray technology.

Total RNA was extracted from *C. elegans* samples using miRNeasy Mini kits (Qiagen, Valencia, CA). Whole genome expression in the *C. elegans* treated with water (control group), 10 μg/ml NaAsO2, 200 μg/ml DMA, 2 μg/ml HgCl2, or 0.5 μg/ml meHgCl for 24 h was determined by using Cellegans_UnrestrictedGE_G2519F_020186 Microarray (Agilent Technologies, Santa Clara, CA). The *C. elegans* genome codes for approximately 20,000 genes (Hillier et al., 2005), and according to the manufacturer, this chip represents $> 18{,}000$ unique genes, providing $> 90\%$ coverage. Sample labeling and microarray processing were performed as detailed in the manufacturer's protocol. The hybridized slides were scanned with an Agilent SureScan DNA Microarray Scanner (Agilent Technologies, Santa Clara, CA) at 3 μm resolution. The resulting images were analyzed by determining the Cy3 fluorescence intensity of all gene spots (features) on each array using the Agilent Feature Extraction Software (Version 11.5). The raw data was uploaded into the ArrayTrack database (Fang et al., 2017). The median fluorescence intensity of all the pixels within one feature was taken as the intensity value for that feature. The raw intensity values were then normalized using 75 percentile channel scaling normalization within ArrayTrack. To identify genes that were differentially expressed between the control group and each experimental group, Benjamini-Hochberg adjusted p-values were calculated (Benjamini and Hochberg, 1995). Genes that passed the 1.5-fold change criterion and had Benjamini-Hochberg adjusted p-value < 0.1 were considered statistically significant. Microarray results are available at https://www.ncbi.nlm.nih.gov/geo/query/acc.cgi?acc = GSE196891.

2.6. Adult native gene expression – Microarray data mining

Standard software tools for differential expression analysis DAVID (Huang da et al., 2009) and Ingenuity Pathway Analysis (QIAGEN Inc., https://digitalinsights.qiagen.com/IPA) yielded little information with the *C. elegans* differentially expressed genes (DEGs). Therefore, two different methods for expression analysis were also utilized, 1. analysis of WormBase generated Expression Clusters and 2. curation (section 2.7). With the first method, sequence identifiers for all DEGs were entered into WormBase's SimpleMine software (WormBase, 2021) for gene ontology (GO) associations, description, expression cluster summary, human homologs, and associated human diseases. DEGs without any information within these parameters were excluded from further analysis. WormBase expression cluster summaries were used to identify DEGs also affected by other chemicals and drugs. To account for variability in the number of DEGs induced by the different conditions, data are presented as a percent or fraction of all DEGs for each test article. Some evaluation was required for inclusion into GO term categories. For the Innate Immune response, search terms 'innate,' 'defense' and 'bacteri' were utilized to screen DEGs for inclusion in this category. The Locomotion category included DEGs with 'loco-

mot' or 'behavior' in the WormBase gene description or GO terms. For the transcriptional regulation (Transcriptional Reg.) category, DEGs with GO terms including 'transcription' and 'histone' were considered for inclusion. The terms 'unfolded,' 'folding,' 'chaperone,' 'heat,' and 'hsp' were used to search for DEGs to include in the Unfolded Protein Response (UPR) category.

2.7. Adult native gene expression – Curated DEGs

In the second method for differential expression analysis, genes with the greatest fold change (the 100 most downregulated for all four conditions and the 100 most upregulated, or all upregulated genes if <100) were further assessed for function. A literature search was conducted for each of these genes to determine if they fit into any patterns or pathways. Unlike the GO term analysis of all DEGs above, in this curated analysis, genes were included in the Immune Resp. category only if they were reported to be regulated by 1.5-fold or more in the same direction with exposure to at least two pathogens or in at least two separate studies, or if RNAi indicated that they were required for microbial defense (Block et al., 2015; Bolz et al., 2010; Engelmann et al., 2011; Evans et al., 2008; Irazoqui et al., 2010; Muir and Tan, 2008; O'Rourke et al., 2006; Pujol et al., 2008; Pukkila-Worley et al., 2011; Ren et al., 2009; Troemel et al., 2006; Wong et al., 2007; Yang et al., 2016). For the Nrf/SKN-1 and DAF-16 response pathway response categories, DEGs were included only if they were shown to be regulated in the same direction by SKN-1 (Hasegawa et al., 2010; Hoeven et al., 2011; Jones et al., 2013; Miller et al., 2011; Oliveira et al., 2009; Park et al., 2009; Przybysz et al., 2009; Steinbaugh et al., 2015; Yanase et al., 2020) or DAF-16 (Kaplan et al., 2019; Kim and Sun, 2007; McElwee et al., 2003; Minniti et al., 2009; Murphy et al., 2003; Nag et al., 2017; Oh et al., 2006; Tepper et al., 2013).

2.8. Adult transgene expression

The parameters of fluorescence, time of flight (TOF, an indicator of size) and extinction (EXT, an indicator of optical density) were assessed with a COPAS™. Green fluorescent protein (GFP) fluorescence was used to measure oxidative stress response (OxStrR, strains LD1171 *gcs-1*p::GFP and CL2166 *gst-4*p::GFP) and unfolded protein response (UPR, strains SJ4003 *aip-1*p::GFP and SJ4005 *hsp-4*p::GFP), while TOF and EXT, which can be adversely affected by toxic substances, were used to define population health for accurate analysis and phenotypic comparison to controls. Because progeny can be excluded from the analysis by gating, FUdR was not used. Compared to the OxStrR biosensor strains used in this study, both UPR transgenic strains were difficult to grow. SJ4003 and SJ4005 took longer to reach L4, and populations were not as abundant as with the wildtype N2 and OxStrR transgenic strains Cl2166 and LD1171, necessitating extra care in baseline phenotype assessment in order to consistently dose at mid-L4. Concentrations tested were determined through range finding experiments. Dosed populations with TOF or EXT morphology values that differed from matched controls by $>$ 20% were excluded from analyses. These changes in morphology parameters were detected at lower concentrations in the UPR strains than in the wild type and OxStrR strains. Because adverse conditions can influence autofluorescence levels, which are not distinguishable from GFP by COPAS, wild-type N2 worms were also evaluated for every condition. Tested concentrations did not affect autofluorescence levels in N2 (data not shown). Data shown are the mean green fluorescence values relative to control and include no effect levels where available up to the highest concentration obtainable that maintained TOF and EXT within 80% of control. Significance was determined from a minimum of three independent experiments per exposure group for Student's T-test p-values * <0.05, ** <0.005.

3. Results

3.1. Developmental toxicity and stage-specific activity changes

C. elegans develop through four distinct larval stages (L1 – L4) prior to adulthood, with a period of inactivity during cuticle molting between each stage. wMicroTrackers (wMTs) use infrared beam interruptions to assess movement within wells of multi-well plates (Simonetta, 2010). Using wMTs, the worm Development and Activity Test (wDAT) tracks these periods of activity and inactivity to simultaneously monitor both the timing of developmental stage acquisition and population locomotor activity levels (Hunt et al., 2018). A wDAT right shift in peak timing indicates developmental delay, and a change in stage-specific peak height indicates hyper- or hypoactivity (Fig. 1A). Over the course of the study, the maximum differences between controls in plates run side by side in the time to reach the 3rd larval stage (L3) peak and the height of L3 peaks was 4% and 5% respectively, providing an indication of assay variability. This experimental variability among negative controls for milestone acquisition timing and stage-specific locomotion is indicated by 0 L-R (Fig. 1B-1E) and was used as a cut-off for wDAT biological significance.

The lowest observed effect level (LOEL) of 6% for delay in the time to reach L3 was observed at 10 μg/ml (76 μM) sodium arsenite (NaAsO2) or 200 μg/ml (1.4 mM) dimethylarsinic acid (DMA). The delay was 13% with 20 μg/ml (154 μM) NaAsO2 or 400 μg/ml (2.8 mM) DMA (Fig. 1B), indicating that about 20 times more DMA was required to achieve the similar levels of developmental delay as with NaAsO2. DMA concentrations that induced 10% to 17% delays in time to reach L3 (300–500 μg/ml) were also associated with reduced population locomotor activity in a dose–response curve from -20% to -39%. There was some hypoactivity with NaAsO2, but the changes were smaller, in the range of -5% to -12%, and not in a dose response pattern (Fig. 1C).

A delay in developmental timing of 5% was observed at 0.5 μg/ml (2 μM) methylmercury chloride (meHgCl) or 2.0 μg/ml (7.5 μM) mercury chloride (HgCl2), and an approximately 16% delay at 2 μg/ml (8 μM) meHgCl or 4 μg/ml (15 μM) HgCl2 (Fig. 1D), indicating that for developmental delay, organic meHgCl is two to four times more toxic than inorganic HgCl2. At 1.0 to 3.0 μg/ml meHgCl, concentrations above the LOEL for delay, stage specific population locomotor activity levels decreased with dose, from -24% to -53%. There was some hypoactivity with HgCl2, but the effects were smaller (-11% to -18%), and too variable to be considered significant (Fig. 1E). These results indicate that at concentrations relevant to developmental delay, organic forms of arsenic and mercury induce additional modes of toxic action beyond those that affect developmental timing, though there is a two orders of magnitude difference in the range of concentrations at which hypoactivity was detected for DMA vs. meHgCl.

The distinctive patterns seen with the wDAT (Fig. 1A) are dependent on the population in each well progressing synchronously through the four larval stages of development. Asynchronous development results in a wDAT readout without distinguishable peaks and valleys, and *C. elegans* larvae observed by microscopy at a variety of developmental stages at the end of the three-day test (Hunt et al., 2018). This loss of synchronous development occurred in two of four HgCl2 experiments at 5 μg/ml, so data presented are from only two experiments (Fig. 1D-E).

3.2.1. Adult native gene expression – Microarray analysis

Gene expression patterns in *C. elegans* larvae change rapidly as they progress through their developmental stages. Assessment in *C. elegans* larvae of toxic effects on gene expression at test chemical concentrations that also delay development is complicated by larval stage specific gene expression (our unpublished observations). For test chemical

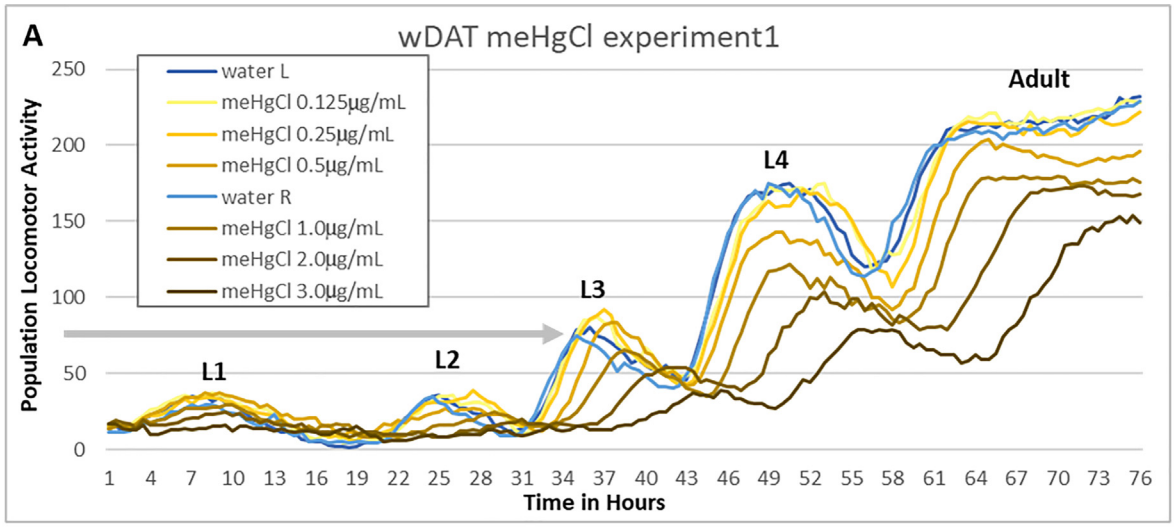

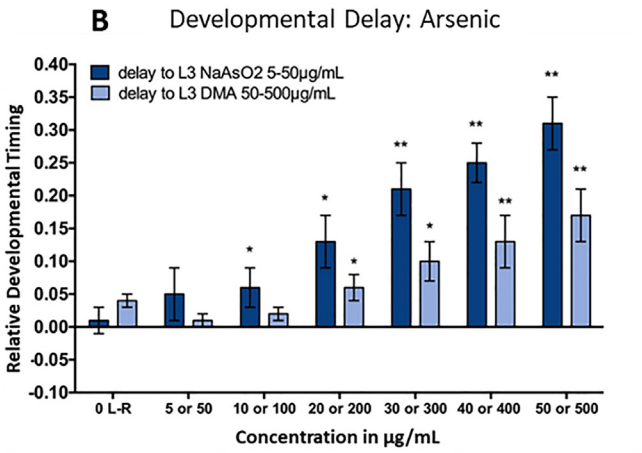

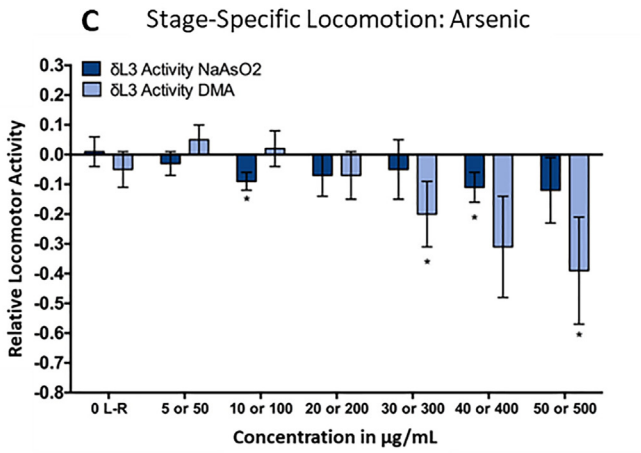

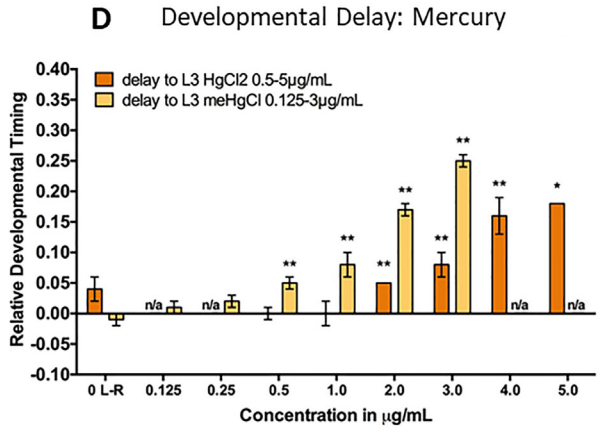

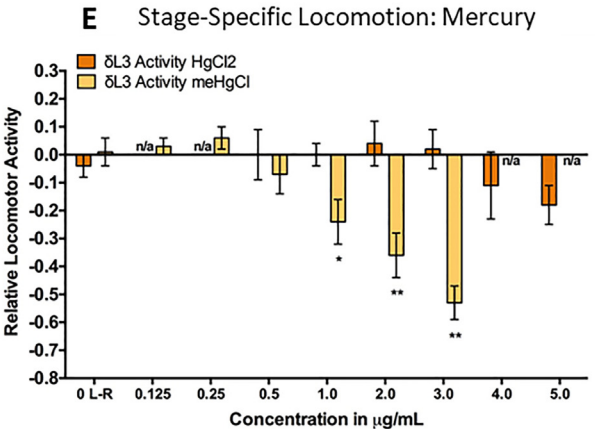

Fig. 1. Developmental toxicity of inorganic vs. organic arsenic and mercury. (A) A representative example of the readout from a single worm Development and Activity Test (wDAT) for methylmercury chloride is shown. The y-axis indicates population locomotor activity levels as measured by mean infrared beam interruption values per well from a single experiment, graphed over half hour time increments on the x-axis. L1 through L4 indicates the four larval stages of *C. elegans* development. There are two separate sets of water controls (L and R), represented by blue and light blue lines for the left and right plates run simultaneously. The horizontal gray arrow from the y-axis indicates the control peak height of the 3rd larval stage (L3). The corresponding times for the two controls to reach the peak height for L3 are 35.5 and 36 h in this experiment. The variability for L3 peak height and timing between controls in separate plates run side-by-side was used as a measure of experimental variability and is shown in 1B-E as '0 L-R'. (B-E) Bars and error bars represent the means and standard deviations from four independent wDAT experiments, with the exception of those for 5.0 µg/mL HgCl2 for which there were data from only two of four experiments. (B&D) The delay in the time to reach L3 relative to controls is plotted. (C&E) L3 locomotor activity peak level relative to controls. Not assessed (n/a). T-test p-values * < 0.05, ** < 0.005. (For interpretation of the references to colour in this figure legend, the reader is referred to the web version of this article.)

specific mode of action evaluation, we therefore exposed adult *C. elegans* for 24 h to concentrations that were equitoxic LOELs for developmental delay in juveniles, 10 μg/ml (76 μM) NaAsO2, 200 μg/ml (1.4 mM) DMA, 2.0 μg/ml (7.5 μM) HgCl2, or 0.5 μg/ml (2 μM) meHgCl.

The results of high-throughput whole genome microarray analyses showed changes in the transcriptome of adult *C. elegans* exposed to NaAsO2, DMA, HgCl2, or meHgCl relative to the water control group. An unsupervised hierarchical clustering of the gene expression data shows that the different treatments could be distinguished by gene expression profile (Fig. 2A). To identify genes that were differentially expressed between the control group and each experimental group, Benjamini-Hochberg adjusted p-values were calculated. Genes that passed 1.5-fold change criterion and had Benjamini-Hochberg adjusted p-value < 0.1 were considered statistically significant.

A total of 927 and 1221 differentially expressed genes (DEGs) were found in *C. elegans* treated with 10 μg/ml NaAsO2 or 200 μg/ml DMA, respectively (Fig. 2B). Interestingly, only 161 DEGs were common for these two chemicals. The treatment with NaAsO2 and DMA induced down-regulation of a greater number of genes in comparison with up-regulated genes, however the organic form of arsenic induced more down-regulated genes than the inorganic arsenic. This was shown by the ratio of down-regulated to up-regulated DEGs of 2.8 for NaAsO2 and 4.5 for DMA.

Adult *C. elegans* exposed to 2 μg/ml HgCl2 or 0.5 μg/ml meHgCl induced 670 and 485 DEGs, respectively. Out of these genes, 154 were commonly expressed by the two treatments. Both chemicals induced a greater number of down-regulated genes in comparison with up-regulated genes, but the organic form of mercury induced a greater number of down-regulated genes than its inorganic form. The ratio of down-regulated/up-regulated DEGs was 5 for HgCl2 and 6.7 for meHgCl (Fig. 2C).

3.2.2. Adult native gene expression – Analysis of all differentially expressed genes

DEGs for each condition were entered into WormBase's SimpleMine software (WormBase, 2021), and all genes for which there was any expression or functional information, 1073 for 200 μg/ml DMA, 721 for 10 μg/ml NaAsO2, 582 for 2.0 μg/ml HgCl2, and 410 for 0.5 μg/ml meHgCl, were included in the following analyses. At tested concentrations, few genes with apoptosis or programmed cell death (Apoptosis/PCD) related GO terms were differentially regulated by the two forms of arsenic (Fig. 3A). In contrast, while the numbers were small, HgCl2 affected the highest proportion of genes in this category. Apoptosis/PCD genes *ced-1* (CEll Death abnormality 1), *drp-1* (Dynamin-Related Protein 1), *dyn-1* (Dynamin 1), *mcd-1* (Modifier of Cell Death phenotype), and apoptotic cell clearance regulator *lst-4* (Almendinger et al., 2011; WormBase, 2021) were all upregulated by HgCl2 (Fig. 3B & Table 2).

From worms to humans, oxidative stress is a major effector of arsenite toxicity due to arsenic's ability to bind with free thiols in proteins and glutathione (Cartwright, 2016; Oliveira et al., 2009; Sahu et al., 2013). Consistent with this, 6–10% of all DEGs upregulated by NaAsO2 or DMA were involved in glutathione related processes (Fig. 3A). Upregulated DEGs in this category for both forms of arsenic included glutathione-s-transferases *gst-10*, *gst-12*, *gst-14*, *gst-16*, *gst-25*, *gst-30*, *gst-35*, and *gsto-2*. Additionally, *gcs-1*, the *C. elegans* ortholog of human GCLC, a subunit of the enzyme that catalyzes the first step in glutathione synthesis (An and Blackwell, 2003) was also upregulated by both forms of arsenic. With the exception of *gst-25*, all of these *gst* genes, as well as *gcs-1*, are upregulated by SKN-1 activity, the *C. elegans* ortholog of mammalian Nrf transcriptional regulators that act in multiple stress resistance pathways, including oxidative stress (Jones et al., 2013; Oliveira et al., 2009; Park et al., 2009; Przybysz et al., 2009). DMA upregulated seven additional *gst* genes unaffected by NaAsO2, as well as oxidative stress response gene *sod-1* (SuperOxide Dismutase 1). At the tested concentrations, no *gst* genes were upregulated by either form of mercury (Fig. 3B). Of note, *gst-19*, which is suppressed by SKN-1 (Miller et al., 2011), was downregulated with both forms of arsenic and by meHgCl (Table 2). Consistent with arsenic inducing oxidative stress, the GO term "oxidation-reduction process" was associated with 7% and 10% of DEGs upregulated by NaAsO2 and DMA, respectively. Genes in this category upregulated by both forms of arsenic included *dhs-8* and K10H10.6, both homologs of human WWOX oxidoreductase, and F30B5.4, a homolog of human OSGIN1 (oxidative stress induced growth inhibitor) (Table 2). In contrast to arsenic, at concentrations tested, the two mercury compounds affected the expression of few, if any, genes with associated glutathione or oxidation–reduction related GO terms.

For heat shock or unfolded protein response (Heat Shock/UPR), though the numbers were small overall, HgCl2 upregulated the highest proportion of DEGs in this category (Fig. 3B), including *dnj-12* and *hsp-3*, homologs of human Hsp40 and Hsp70, respectively. Heat shock genes *hsp-12.1*, *hsp-16.41*, and *hsp-16.48* were downregulated by DMA, HgCl2, and NaAsO2, respectively. HgCl2 and meHgCl both downregulated *dve-1*, a transcription factor involved in chaperone binding and mitochondrial UPR (Tian et al., 2016).

Exposure to arsenic or mercury alters mitogen-activated protein kinase (MAPK) pathway activity in human cells, rodents, and *C. elegans* (Aguado et al., 2013; Hao et al., 2009; Inoue et al., 2005; Wyatt et al., 2017; Yang and Frenkel, 2002). Consistent with a previous report of *C. elegans* MAPK pathway genes *sek-1* and *pmk-1* being downregulated with meHgCl and HgCl2 exposure (Wyatt et al., 2017), in this study *mig-15*, *pde-6*, and *unc-4* were downregulated by one or both forms of mercury. In contrast, human MAP2K7 homolog *jkk-1* was upregulated, but only by HgCl2 (Table 2). No MAPK pathway genes were altered by either form of arsenic. However, *mbl-1*, the sole *C. elegans* ortholog of mammalian Muscleblind-like proteins and MAPK regulator (Matilainen et al., 2021), was upregulated by DMA but downregulated by NaAsO2.

Arsenic is a known immune modulator in mammals (Dangleben et al., 2013). Consistent with this, GO terms related to immune function including 'innate immune response,' 'defense response to bacterium,' and 'defense response to fungus,' were associated with 7–8% of genes upregulated by NaAsO2 and DMA, while few genes affected by the two mercury species fell in this category. DEGs with locomotion related GO terms or WormBase descriptions were associated with 9% of DEGs upregulated by HgCl2 including *ldb-1*, involved in mechanosensory behavior, and *snf-6*, used to study Duchenne muscular dystrophy (WormBase, 2021). DEGs with the GO term "metal ion binding" were induced and inhibited to a similar extent by the two forms of arsenic (Fig. 3A). In contrast, 14% of genes upregulated by HgCl2 were in this category while no DEGs upregulated by meHgCl had "metal ion binding" as a GO term (Fig. 3B).

The GO term "signal transduction" was associated with about 4% of the DEGs upregulated by the two forms of arsenic versus 8–9% of DEGs upregulated by the two forms of mercury. Genes in this category included *avr-14*, an extracellular glutamate-gated chloride channel subunit upregulated by NaAsO2, DMA and HgCl2, and *daf-38*, a neuronal G protein-coupled receptor upregulated by NaAsO2, DMA and meHgCl (WormBase, 2021). Both forms of mercury downregulated *mig-15* and *rgef-1*, involved in MAPK and Ras signaling, respectively. A regulator of Rho protein signal transduction, *gei-1*, was also downregulated by both HgCl2 and meHgCl. Additionally, several insulin genes were in the signal transduction category, including *ins-2*, downregulated by NaAsO2, DMA, and HgCl2, and *ins-5* which was affected by all four conditions (Table 2).

For genes with GO terms or WormBase descriptions relating to transcriptional regulation and/or histone modification (Transcriptional

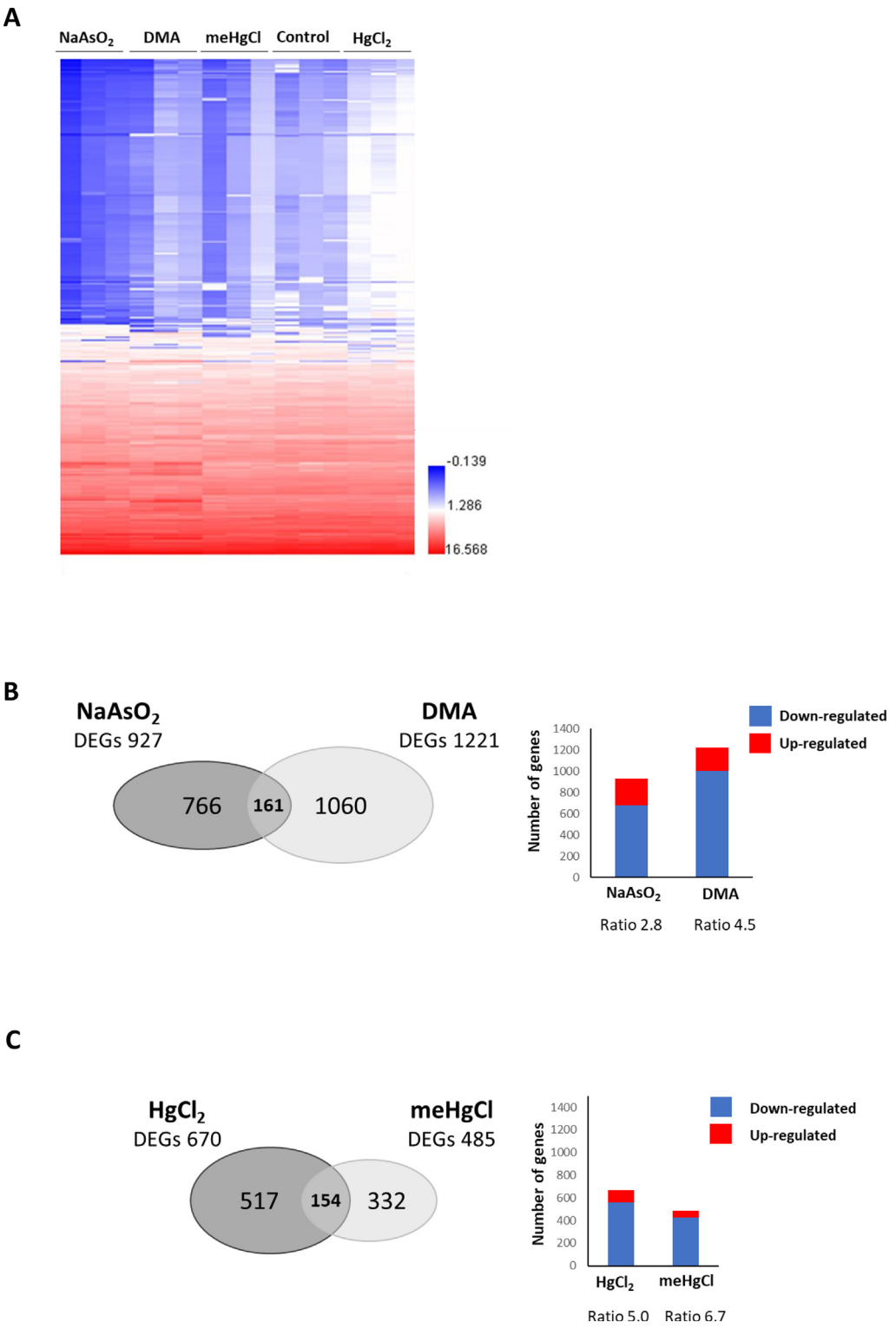

Fig. 2. Microarray analysis of gene expression with inorganic vs. organic arsenic and mercury. Whole-genome microarray transcriptomic analysis of *C. elegans* exposed to 10 μg/ml NaAsO2, 200 μg/ml DMA, 0.5 μg/ml meHgCl, or 2.0 μg/ml HgCl2. A) Heat maps illustrating differences in global gene expression profiles between control and exposed adult *C. elegans*. B) Venn diagram illustrating the number of differentially expressed genes and their analysis in *C. elegans* exposed to NaAsO2 or DMA. C) Venn diagram illustrating the number of differentially express genes and their analysis in *C. elegans* exposed to meHgCl or HgCl2.

Reg.), the two forms of mercury induced proportionally more DEGs than did the two forms of arsenic, and this was also true for DEGs with known or predicted nuclear localization of their gene product (Fig. 3). Predicted transcription factor *tab-1* (Touch Abnormal), homologous to human BSX, was downregulated by all four conditions (Table 2). Known or predicted transcription factors *daf-3*, *nhr-147*, *nhr-150*, *nhr-171*, *npax-1*, and Y111B2A.10 were all downregulated by DMA, HgCl2 and meHgCl. Transcriptional regulator *pha-2* was downregulated by NaAsO2, DMA, and meHgCl. Regulators of transcription by RNA polymerase II *ceh-5*, *fkh-8*, *hlh-34*, and *nhr-127* were downregu-

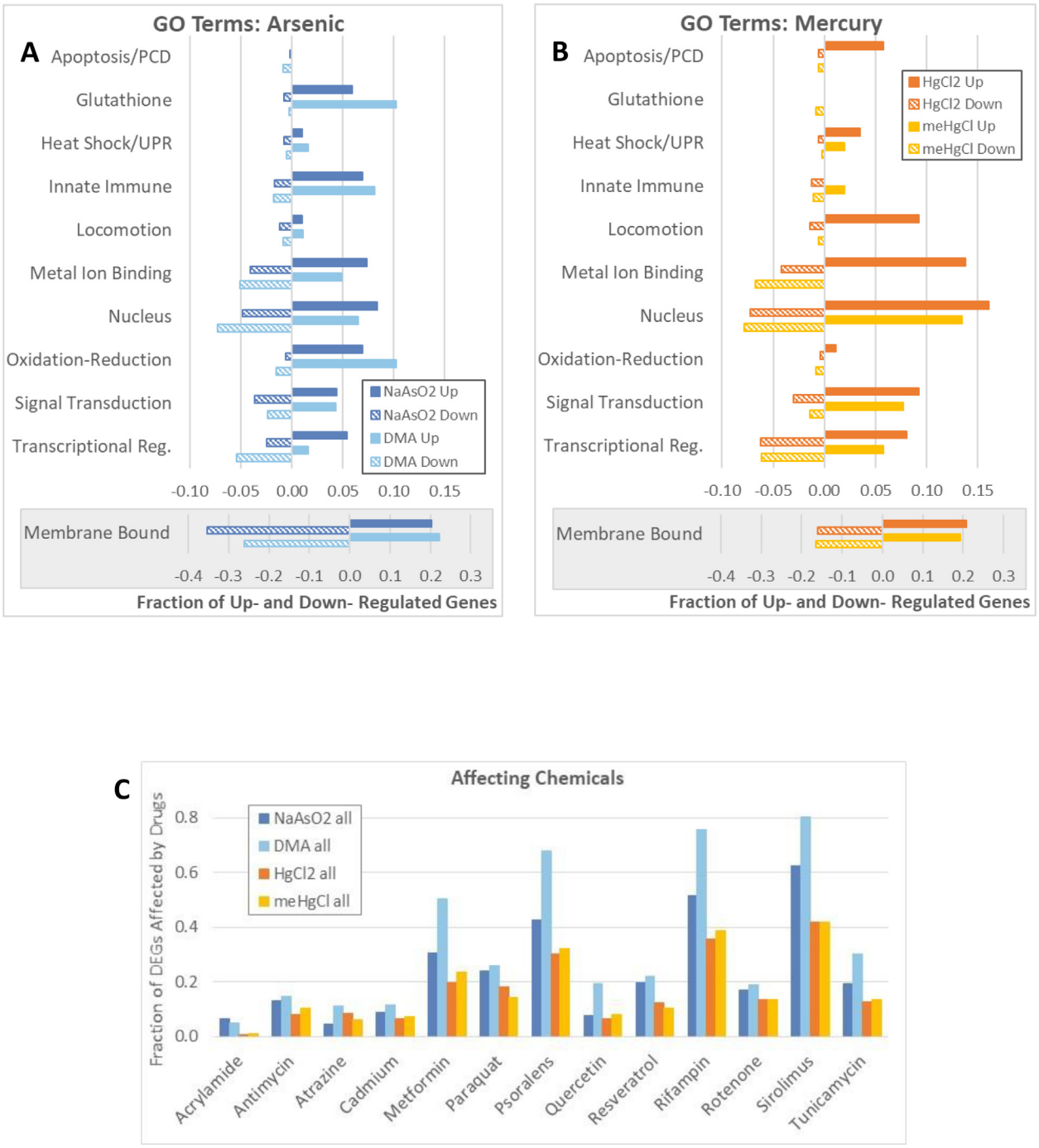

Fig. 3. Gene Ontology (GO) terms, and genes also affected by other chemicals. WormBase's GO terms and descriptions relating to specific functions were used to assign into categories all differentially expressed genes (DEGs) for which there was expression, function, and/or homology information in WormBase. (A-B) The number of DEGs varied among conditions, therefore bars represent the fraction of all DEGs that were in each category. Many DEGs fell into multiple categories and were therefore counted more than once. Note that the fraction of DEGs with the GO term "integral component of membrane" (Membrane Bound) are shown with a different scale. (C) The fraction of DEGs (y-axis) also altered by exposure to listed drugs (x-axis) is graphed. WormBase's expression cluster summary only indicates that a gene's expression is affected by a chemical, but not in which direction, therefore the fraction of DEGs also affected by various chemicals is presented for up- and downregulated DEGs together. Abbreviations: Upregulated (Up), Downregulated (Down), Programmed Cell Death (PCD), Unfolded Protein Response (UPR), Transcriptional Regulation plus Histone Modification (Transcriptional Reg.).

lated by both DMA and meHgCl. Controllers of DNA and transcription factor binding *bro-1*, *ceh-16*, *ref-2* and *nhr-187* were downregulated by both DMA and HgCl2. Both DMA and NaAsO2 upregulated suppressors of RNA polymerase II activity *cfi-1* and *wdr-23*, and downregulated transcriptional activator *hlh-17*. HgCl2 and meHgCl downregulated transcriptional regulator *nhr-188*. Several of the genes in this category affect histone methylation, including *jmjd-3.2* and *jmjd-1.1* (Agger et al., 2007; Lee et al., 2015), histone demethylases downregulated by DMA and HgCl2, respectively. NaAsO2 upregulated *dot-1.2* and *met-1*, genes predicted to encode histone methyltransferases (Andersen and Horvitz, 2007; Cecere et al., 2013), and *gei-8*, a histone deacetylase and transcription repressor (Mikoláš et al., 2013). Overall,

Table 2
Categorized Differentially Regulated Genes.

sequence	gene name	human homolog(s)	NaAsO2	DMA	HgCl2	meHgCl	category	references
PAR2.3	*aak-1*	PRKAA1, PRKAA2	–	–	–	1.5	AMPK, hhDG	(Kuo et al., 2020; Narbonne and Roy, 2009; WormBase, 2021)
ZK909.2	*kin-1*	PRKACA	−1.8	−1.8	−1.7	–	AMPK	(WormBase, 2021)
K09E9.4	–	PKIA, PKIB, PKIG	–	–	−1.7	−2.0	AMPK	(WormBase, 2021)
ZK1320.4	*cyp-13A10*	CYP3A4, CYP3A43	–	−2.1	−1.8	−2.0	CYP, hhDG, mib	(WormBase, 2021)
T10B9.5	*cyp-13A3*	CYP3A4, CYP3A43	−1.8	–	–	–	CYP, hhDG, mib	(WormBase, 2021)
K09A11.3	*cyp-14A2*	CYP2U1	–	−2.1	–	–	CYP, hhDG, mib	(WormBase, 2021)
K09A11.4	*cyp-14A3*	CYP2U1	–	−1.8	–	–	CYP, hhDG, mib	(WormBase, 2021)
R04D3.1	*cyp-14A4*	CYP2U1	–	4.6	–	–	CYP, iIR, hhDG, mib	(Engelmann et al., 2011; WormBase, 2021)
T10H4.10	*cyp-34A1*	CYP2U1	–	−2.5	–	–	CYP, DrugR hhDG, mib	(WormBase, 2021)
K09D9.2	*cyp-35A3*	CYP2U1	–	−2.7	–	–	CYP, DrugR, hhDG, mib	(WormBase, 2021)
C49G7.8	*cyp-35A4*	CYP2U1	1.6		–	–	CYP, DrugR, hhDG, mib	(WormBase, 2021)
K07C6.2	*cyp-35B3*	CYP2U1	–	1.9	–	–	CYP, DrugR, hhDG, mib	(WormBase, 2021)
F14H3.10	*cyp-35D1*	CYP2U1	–	5.6	–	–	CYP, iIR, DrugR, hhDG, mib	(Troemel et al., 2006; Wong et al., 2007; WormBase, 2021)
F01D5.9	*cyp-37A1*	–	–	–	–	−1.5	CYP	(WormBase, 2021)
F55A8.2d	*egl-4*	PRKG1	–	–	−1.8	–	DAF-2/IIS, Loco, hhDG, mib	(WormBase, 2021)
ZK1251.2	*ins-7*	–	−1.9	−1.9	–	–	DAF-2/IIS, rSKN-1	(Murphy et al., 2003; Oliveira et al., 2009)
H42K12.1b	*pdk-1*	PDPK1	–	1.5	1.5	–	DAF-2/IIS, hhDG, OxStrR	(WormBase, 2021)
B0454.7	*clec-2*	–	7.1	1.8	–	–	rDAF-16	(Nag et al., 2017; WormBase, 2021)
F55G11.5	*dod-22*	–	–	−4.2	–	–	rDAF-16	(Tepper et al., 2013; Watanabe et al., 2020)
F37F2.3	*gst-25*	GSTP1	6.9	10.4	–	–	rDAF-16, hhDG	(Minniti et al., 2009)
R02D3.6	*grl-19*	–	–	2.3	–	1.6	rDAF-16, OxStrR	(Kim and Sun, 2007)
ZK75.2	*ins-2*	–	−1.6	−2.2	−1.8	–	rDAF-16	(Murphy et al., 2003)
R02D3.1	*aass-1*	AASS	–	–	1.6	–	hhDG	(WormBase, 2021)
Y74C10AR.3	*abtm-1*	ABCB7	–	–	1.6	–	hhDG, OxStrR	(Gonzalez-Cabo et al., 2011; WormBase, 2021)
T11B7.4	*alp-1*	LDB3, PDLIM5	–	–	–	−2.0	hhDG	(WormBase, 2021)
Y71G12B.1	*chaf-2*	CHAF1B	–	–	–	1.6	hhDG	(WormBase, 2021)
E04F6.11	*clh-3*	CLCN2	–	–	1.7	–	hhDG	(WormBase, 2021)
ZC116.3	*cubn-1*	CUBN	−2.7	−1.7	–	−2.5	hhDG	(WormBase, 2021)
F11H8.4	*cyk-1*	DIAPH1, DIAPH2	–	–	–	−2.3	hhDG	(WormBase, 2021)
ZC477.9	*deb-1*	VCL	–	–	1.6	–	hhDG	(WormBase, 2021)
T12E12.4	*drp-1*	DNM1L	–	–	1.6	–	hhDG	(WormBase, 2021)
F43G9.6	*fer-1*	DYSF	2.5	−1.5	–	–	hhDG	(WormBase, 2021)
ZK180.1	*gbb-2*	GABBR2	–	−2.1	–	–	hhDG, DrugR	(WormBase, 2021)
F45H7.2	*gei-1*	DLC1, STARD13	–	–	−2.1	−2.1	hhDG	(WormBase, 2021)
F54D7.3	*gnrr-1*	GNRHR	–	–	1.8	–	hhDG	(WormBase, 2021)
R03E9.4	*irk-1*	KCNJ14, KCNJ4	–	2.1	–	–	hhDG	(WormBase, 2021)
R13A1.2	*kcc-1*	SLC12A4, SLC12A6	–	–	−2.1	–	hhDG	(WormBase, 2021)
M01B2.1	*kin-30*	KIT, PDGFRA	–	–	–	−3.3	hhDG	(WormBase, 2021)
B0457.1	*lat-1*	ADGRL3	1.6	–	1.7	–	hhDG	(WormBase, 2021)
R05C11.3	*mca-2*	ATP2B2, ATP2B3	–	–	1.5	–	hhDG	(WormBase, 2021)
F32D1.10	*mcm-7*	MCM7	–	–	–	1.5	hhDG, DNArep	(WormBase, 2021)
F20B6.3	*mrp-6*	ABCC4	–	–	–	2.7	hhDG	(WormBase, 2021)
Y43F8C.12	*mrp-7*	ABCC2	1.9	–	1.8	1.8	hhDG	(WormBase, 2021)
T22E5.5.1	*mup-2*	TNNT1, TNNT3	–	–	1.6	–	hhDG	(WormBase, 2021)
Y37A1C.1	*nkcc-1*	SLC12A2 SLC12A3	–	–	1.5	–	hhDG	(WormBase, 2021)
F31B9.1	*npr-33*	AGTR1, GPR15	–	–	−2.3	–	hhDG	(WormBase, 2021)
C01F6.6	*nrfl-1*	SLC9A3R1	–	–	1.6	–	hhDG	(WormBase, 2021)
H12C20.2	*pms-2*	PMS2	–	–	–	−2.5	hhDG, DNArep	(WormBase, 2021)
K07A3.2	*ptr-12*	PTCHD3	–	–	–	2.0	hhDG	(WormBase, 2021)
Y18D10A.7	*ptr-17*	PTCHD3	–	–	–	2.1	hhDG	(WormBase, 2021)
F25H5.3	*pyk-1*	PKLR, PKM	–	–	1.9	–	hhDG, mib	(WormBase, 2021)
T08B2.5	*rbm-5*	RBM10, RBM5	–	–	1.7	–	hhDG, mib	(WormBase, 2021)
F25B3.3	*rgef-1*	RASGRP3	–	–	−2.8	−3.1	hhDG	(WormBase, 2021)
C06E1.10	*rha-2*	DHX37	–	–	1.8	–	hhDG	(WormBase, 2021)
T01H8.1	*rskn-1*	RPS6KA1, RPS6KA2	–	–	1.5	–	hhDG	(WormBase, 2021)

(*continued on next page*)

Table 2 (*continued*)

sequence	gene name	human homolog(s)	NaAsO2	DMA	HgCl2	meHgCl	category	references
C06E7.1	*sams-3*	MAT1A, MAT2A	–	–	1.7	–	hhDG, mib	(WormBase, 2021)
K11G12.3	*smf-2*	SLC11A1, SLC11A2	–	–	–	−2.1	hhDG	(WormBase, 2021)
H21P03.3	*sms-1*	SGMS2	–	–	1.5	–	hhDG	(WormBase, 2021)
F55H12.1	*snf-2*	SLC6A11, SLC6A6	–	–	–	2.1	hhDG	(WormBase, 2021)
Y46G5A.30	*snf-5*	SLC6A8, SLC6A12	2.1	–	–	–	hhDG, mib	(WormBase, 2021)
Y48E1B.14	*snx-14*	SNX14	–	–	1.9	–	hhDG	(WormBase, 2021)
T19H12.11	*ugt-10*	UGT1A9, UGT2B28	4.5	–	–	–	hhDG	(WormBase, 2021)
F29F11.2	*ugt-34*	UGT1A8, UGT2B15	94.5	–	–	–	hhDG	(WormBase, 2021)
ZK1151.1	*vab-10*	DST	1.7	2.0	–	2.9	hhDG	(WormBase, 2021)
T08G11.1	–	VPS13A	–	–	1.7	–	hhDG	(WormBase, 2021)
Y37A1A.4	–	RIPOR2, RIPOR3	−1.5	–	–	−1.8	hhDG	(WormBase, 2021)
Y48G1C.10	–	MTMR10, MTMR12	–	–	–	1.6	hhDG	(WormBase, 2021)
Y71H10B.1	–	NT5C2	–	–	1.6	–	hhDG, OxStrR	(Wang et al., 2010; WormBase, 2021)
ZK1073.1	–	NDRG1, NDRG2	–	–	1.5	–	hhDG	(WormBase, 2021)
R05F9.12	*aagr-2*	MGAM	–	–	1.6	–	iIR, hhDG	(Engelmann et al., 2011; WormBase, 2021)
K02G10.7	*aqp-8*	AQP9	–	2.2	–	–	iIR	(Irazoqui et al., 2010; O'Rourke et al., 2006; WormBase, 2021)
ZK896.7	*clec-186*	–	–	–	–	−1.9	iIR, rMAPK	(Block et al., 2015; WormBase, 2021)
C41H7.7	*clec-3*	–	9.9	5.8	–	–	iIR	(Engelmann et al., 2011; Evans et al., 2008; Muir and Tan, 2008; Troemel et al., 2006)
Y46C8AL.3	*clec-70*	–	–	−8.6		−5.6	iIR	(WormBase, 2021)
F58E6.7	*hrg-3*	–	−1.9	−2.3	−1.9	−2.0	iIR	(Engelmann et al., 2011; WormBase, 2021)
F26A1.10	*nspd-9*		1.5	2.1	–	–	iIR	(Engelmann et al., 2011)
C05A9.1	*pgp-5*	ABCB1	–	−2.3	–	–	iIR, DrugR	(WormBase, 2021)
C05C10.4	*pho-11*	–	1.6	2.2	–	–	iIR, rDAF-16	(Bolz et al., 2010; McElwee et al., 2003; Troemel et al., 2006; Wong et al., 2007)
C43H6.6	–	–	–	–	–	1.7	iIR	(Engelmann et al., 2011)
F01D5.2	–	–	4.9	3.1	–	–	iIR	(Engelmann et al., 2011; Ren et al., 2009; Troemel et al., 2006)
F26D2.3	–	GCNT1, GCNT3	–	–	–	2.0	iIR, hhDG	(Engelmann et al., 2011; WormBase, 2021)
F47B3.7	–	–	–	2.6	–	–	iIR	(Engelmann et al., 2011; Wong et al., 2007)
F48E3.9	–	–	2.2	–	–	–	iIR	(Engelmann et al., 2011)
H12I13.5	–	–	1.8	–	–	1.7	iIR	(Engelmann et al., 2011)
K02D3.1	–	–	−3.3	–	–	–	iIR	(Irazoqui et al., 2010; Troemel et al., 2006)
R04B5.11	–	–	–	2.6	–	–	iIR	(Engelmann et al., 2011)
R09H10.5.2	–	–	–	–	2.1	–	iIR	(Engelmann et al., 2011)
T01B6.1	–	SAPCD2	2.1	–	–	–	iIR	(Engelmann et al., 2011)
T28A11.2	–	–	–	3.6	–	–	iIR	(Engelmann et al., 2011)
B0207.12	*avr-14*	GLRA3, GLRA4	2.0	2.6	1.6	–	Loco, DrugR	(WormBase, 2021)
K04F10.4	*bli-4*	PCSK5, PCSK6	−1.5	–	–	–	Loco, hhDG	(WormBase, 2021)
F46C8.5	*ceh-14*	LHX-3, LHX4	–	–	−1.7	–	Loco, TxR, hhDG, mib	(WormBase, 2021)
C55B7.12	*che-1*	ZNF500	–	−2.6	–	–	Loco, TxR, mib	(WormBase, 2021)
Y41C4A.4	*crh-1*	ATF1, CREB1, CREM	–	–	−2.5	–	Loco, TxR, hhDG	(WormBase, 2021)
F15A8.5	*dop-1*	DRD1, DRD5	–	1.6	–	–	Loco, hhDG	(WormBase, 2021)
C16C2.2	*eat-16*	RGS9, RGS11	–	–	−1.6	–	Loco, hhDG	(WormBase, 2021)
C06A12.4	*gcy-27*	GUCY2D	–	–	−2.2	–	Loco, hhDG	(WormBase, 2021)
T15H9.3	*hlh-6*	ASCL3	–	−1.8	–	–	Loco, TxR	(WormBase, 2021)
F58A3.1	*ldb-1*	LDB1, LDB2	–	–	1.6	–	Loco, TxR, rDAF-16	(Oh et al., 2006; WormBase, 2021)
T07H8.4	*mec-1*	–	−1.5	−1.7	1.5	–	Loco	(WormBase, 2021)
E01F3.1	*pde-3*	PDE3A	−1.6	–	–	–	Loco, TxR, hhDG	(WormBase, 2021)
Y11D7A.4	*rab-28*	RAB28	–	−2.4	–	–	Loco, hhDG	(WormBase, 2021)
M01G5.5	*snf-6*	SLC6A5, SLC6A14	–	–	1.6	–	Loco, hhDG	(WormBase, 2021)
C18A3.5	*tiar-1*	TIA1, TIAL1	–	–	1.9	–	Loco, OxStrR	(WormBase, 2021)
F56A12.1	*unc-39*	SIX4, SIX6	–	−1.9	–	–	Loco, TxR, hhDG	(WormBase, 2021)
ZC101.2	*unc-52*	HSPG2	−1.6	–	–	–	Loco, hhDG	(WormBase, 2021)
C11D2.6	*unc-77*	NALCN	–	–	–	−2.0	Loco	(WormBase, 2021)
C09D1.1	*unc-89*	SPEG	–	–	−1.6	–	Loco, hhDG	(WormBase, 2021)
F35C8.3	*jkk-1*	MAP2K7	–	–	1.9	–	MAPK, Loco, mib	(WormBase, 2021)
K02H8.1	*mbl-1*	MBNL1, MBNL2	−2.0	1.9	–	–	MAPK, TIR, hhDG, mib	(Matilainen et al., 2021; WormBase, 2021)

Table 2 (*continued*)

sequence	gene name	human homolog(s)	NaAsO2	DMA	HgCl2	meHgCl	category	references
ZC504.4	*mig-15*	MINK1, TNIK	–	–	−1.9	−2.1	MAPK, hhDG	(WormBase, 2021)
Y95B8A.10	*pde-6*	PDE8A, PDE8B	–	–	–	−2.2	MAPK, hhDG, mib	(WormBase, 2021)
K11E8.1	*unc-43*	CAMK2D	–	–	−2.0	–	MAPK, TxR, hhDG, mib	(WormBase, 2021)
W02G9.2.3	*kel-8*	KLHL8	–	–	–	1.6	rMAPK	(Cui et al., 2007)
F21F8.4	*asp-12*	CTSE, PGA4, PGC	–	−1.9	–	−1.5	PCD	(WormBase, 2021)
Y39B6A.23	*asp-16*	CTSE, PGA4, PGC	–	−2.3	–	–	PCD	(WormBase, 2021)
Y47H9C.4	*ced-1*	MEGF10, MEGF11	–	–	1.5	–	PCD, UPR, iIR, hhDG	(Haskins et al., 2008; WormBase, 2021)
F08F1.5	*ced-8*	XKR4, XKR6, XKR7	–	−1.5	–	–	PCD	(WormBase, 2021)
C09G12.8	*ced-10*	RAC1, RAC2	–	–	−1.6	–	PCD, hhDG	(WormBase, 2021)
F43G9.11	*ces-1*	SCRT1, SCRT2	–	−3.4	–	–	PCD, TxR	(WormBase, 2021)
ZK909.4	*ces-2*	DBP,TEF	–	−3.4	–	–	PCD, TxR, hhDG	(WormBase, 2021)
T21H3.3	*cmd-1*	CALM1	–	–	−1.5	–	PCD, hhDG, mib	(WormBase, 2021)
T12E12.4	*drp-1*	DNM1L	–	–	1.6	–	PCD, hhDG	(WormBase, 2021)
C02C6.1	*dyn-1*	DNM1, DNM2	–	–	1.5	–	PCD, Loco, hhDG	(WormBase, 2021)
C49A1.4	*eya-1*	EYA1, EYA2, EYA4	–	−1.7	–	–	PCD, TxR, OxStrR, Loco, UPR, DNArep, hhDG, mib	(WormBase, 2021)
M05B5.5	*hlh-2*	TCF3, TCF4, TCF12	−1.7	–	–	–	PCD, TxR, hhDG	(WormBase, 2021)
Y37A1B.2	*lst-4*	SNX18, SNX33	–	–	1.9	–	PCD	(WormBase, 2021)
Y51H1A.6	*mcd-1*	–	–	–	1.6	–	PCD, mib	(WormBase, 2021)
C33A11.1	*nfki-1*	NFKBIZ	–	–	1.5	–	PCD, TxR	(WormBase, 2021)
ZK524.1	*spe-4*	–	–	−1.7	–	–	PCD, Notch	(WormBase, 2021)
F11F1.7	*ttr-52*	–	–	−2.4	−2.0	−1.8	PCD	(WormBase, 2021)
T19E7.2	*skn-1*	NFE2L1, NFE2L2, NFE2L3	–	–	–	1.5	SKN-1, TxR, OxStrR, UPR, iIR, rMAPK, hhDG	(WormBase, 2021)
K10C2.3	*asp-14*	CTSE, PGA3	2.3	2.3	–	–	rSKN-1, iIR, rAMPK, rMAPK	(Bolz et al., 2010; Oliveira et al., 2009; Shin et al., 2011; Troemel et al., 2006; WormBase, 2021)
C12C8.2	*cbl-1*	–	2.1	–	–	–	rSKN-1, iIR	(Engelmann et al., 2011; Oliveira et al., 2009)
F35E8.11	*cdr-1*	FAXC	–	5.0	–	–	rSKN-1, iIR, rDAF-16,	(Engelmann et al., 2011; Evans et al., 2008; McElwee et al., 2003; Oliveira et al., 2009; Troemel et al., 2006; WormBase, 2021)
ZK666.6	*clec-60*	–	−2.2	−2.2	–	–	rSKN-1, iIR	(Oliveira et al., 2009; WormBase, 2021)
ZK673.9	*clec-143*	–	2.8	–	–	–	rSKN-1, iIR	(Engelmann et al., 2011; Oliveira et al., 2009; Troemel et al., 2006)
K10B2.2	*ctsa-4.1*	CTSA	1.9	–	–	–	rSKN-1, iIR	(Engelmann et al., 2011; Oliveira et al., 2009; Troemel et al., 2006; Wong et al., 2007)
F02C12.5	*cyp-13B1*	CYP3A4, CYP3A5	–	−3.0	–	–	rSKN-1, CYP, hhDG, mib	(WormBase, 2021)
K10H10.3	*dhs-8*	WWOX	1.8	4.3	–	–	rSKN-1, hhDG	(Oliveira et al., 2009; WormBase, 2021)
K10D11.1	*dod-17*	–	6.4	2.6	–	–	rSKN-1, iIR	(Engelmann et al., 2011; Oliveira et al., 2009; Troemel et al., 2006; WormBase, 2021)
C32H11.12	*dod-24*	–	5.3	1.7	–	–	rSKN-1, iIR	(Block et al., 2015; Bolz et al., 2010; Oliveira et al., 2009; Troemel et al., 2006; WormBase, 2021)
Y4C6B.6	*gba-4*	GBA	–	–	–	−4.7	rSKN-1, iIR, hhDG	(Paek et al., 2012; WormBase, 2021; Zárate-Potes et al., 2020)
F37B12.2	*gcs-1*	GCLC	1.8	1.6	–	–	rSKN-1, OxStrR	(Hasegawa et al., 2008; Oliveira et al., 2009; WormBase, 2021)
R107.7	*gst-1*	GSTP1	1.6	1.7	–	–	rSKN-1, UPR, hhDG	(Oliveira et al., 2009; Settivari et al., 2013)
R03D7.6	*gst-5*	HPGDS	–	3.0	–	–	rSKN-1, iIR	(Evans et al., 2008; Oliveira et al., 2009; Troemel et al., 2006; Wong et al., 2007)
F11G11.3	*gst-6*	HPGDS	–	1.8	–	–	rSKN-1	(Oliveira et al., 2009; WormBase, 2021)
F11G11.2	*gst-7*	HPGDS	–	1.5	–	–	rSKN-1	(Oliveira et al., 2009; WormBase, 2021)
F11G11.1	*gst-8*	HPGDS	–	1.6	–	–	rSKN-1	(Oliveira et al., 2009; WormBase, 2021)
Y45G12C.2	*gst-10*	GSTP1	2.1	2.1	–	–	rSKN-1, OxStrR, hhDG	(Oliveira et al., 2009; Park et al., 2009; Tullet et al., 2008; WormBase, 2021)
F37B1.2	*gst-12*	HPGDS	3.8	5.9	–	–	rSKN-1, OxStrR	(Oliveira et al., 2009; Park et al., 2009; VanDuyn et al., 2010)
T26C5.1	*gst-13*	HPGDS	1.6	2.0	–	–	rSKN-1, iIR	(Oliveira et al., 2009; Park et al., 2009; Troemel et al., 2006; WormBase, 2021)
F37B1.3	*gst-14*	HPGDS	2.8	4.0	–	–	rSKN-1, iIR, OxStrR	(Engelmann et al., 2011; Oliveira et al., 2009; Park et al., 2009)
F37B1.5	*gst-16*	HPGDS	5.8	6.8	–	–	rSKN-1	(Przybysz et al., 2009)
F37B1.8	*gst-19*	HPGDS	−2.2	−2.2	–	−3.2	rSKN-1	(Oliveira et al., 2009)
ZK546.11	*gst-30*	HPGDS	5.3	7.5	–	–	rSKN-1	(Przybysz et al., 2009)
Y1H11.2	*gst-35*	HPGDS	2.1	6.4	–	–	rSKN-1	(Oliveira et al., 2009)
C02D5.3	*gsto-2*	GSTO1,	4.1	5.3	–	–	rSKN-1, OxStrR	(Oliveira et al., 2009; WormBase, 2021)

(*continued on next page*)

Table 2 (*continued*)

sequence	gene name	human homolog(s)	NaAsO2	DMA	HgCl2	meHgCl	category	references
		GSTO2						
ZK84.3	*ins-5*	–	1.8	2.3	−1.8	2.3	rSKN-1, rMAPK, rDAF-16	(Kaplan et al., 2019; Yanase et al., 2020)
F35E12.5	*irg-5*	–	1.9	2.7	–	–	rSKN-1, iIR, rMAPK	(Bolz et al., 2010; Foster et al., 2020; O'Rourke et al., 2006; Oliveira et al., 2009; Pukkila-Worley et al., 2011; Wan et al., 2021)
T22G5.6	*lbp-8*	FABP5, PMP2	–	7.2	–	–	rSKN-1, hhDG	(Steinbaugh et al., 2015)
K08H10.2	*lea-1*	PLIN4	–	–	1.5	–	rSKN-1, rUPR	(Oliveira et al., 2009; WormBase, 2021)
ZK1058.6	*nit-1*	–	3.6	2.2	–	–	rSKN-1, rMAPK	(Miller et al., 2011; Oliveira et al., 2009)
H12D21.1	*nspa-1*	–	10.7	8.7	–	–	rDAF-16	(McElwee et al., 2003)
ZC412.6	*nspa-5*	–	9.4	7.5	–	–	rSKN-1, iIR	(Engelmann et al., 2011; Oliveira et al., 2009)
W06A7.5	*nspa-8*	–	34.0	21.8	–	–	rSKN-1	(Oliveira et al., 2009)
F57C9.1	*pdxk-1*	PDXK	2.0	2.0	–	–	rSKN-1, mib	(Oliveira et al., 2009; WormBase, 2021)
C55A6.5	*sdz-8*	CBR3	–	2.2	–	–	rSKN-1	(Oliveira et al., 2009)
C15F1.7	*sod-1*	SOD1	–	1.7	–	–	rSKN-1, OxStrR, mib	(Park et al., 2009; WormBase, 2021)
H23N18.1	*ugt-13*	UGT1A1, UGT2B28, UGT2B7	2.3	–	–	–	rSKN-1, iIR, hhDG	(Engelmann et al., 2011; Hasegawa et al., 2010; Jones et al., 2013; Troemel et al., 2006)
B0348.2	–	–	−1.5	−1.9	–	–	rSKN-1, mib	(Oliveira et al., 2009; WormBase, 2021)
C17H12.6	–	–	2.2	–	–	–	rSKN-1, iIR	(Engelmann et al., 2011; Oliveira et al., 2009; Troemel et al., 2006)
C32H11.3	–	–	10.1	6.6	–	–	rSKN-1, iIR	(Engelmann et al., 2011; Oliveira et al., 2009; Troemel et al., 2006)
C32H11.4	–	–	11.7	6.7	–	–	rSKN-1, iIR	(Muir and Tan, 2008; Oliveira et al., 2009; Yang et al., 2016)
F01D5.3	–	–	3.4	3.3	–	–	rSKN-1, iIR	(Oliveira et al., 2009; Ren et al., 2009)
F01D5.5	–	–	2.9	–	–	–	rSKN-1, iIR	(O'Rourke et al., 2006; Oliveira et al., 2009; Ren et al., 2009; Troemel et al., 2006)
F39B2.3	–	CRYZ	1.9	2.0	–	–	rSKN-1, T*l*R	(Oliveira et al., 2009; WormBase, 2021)
F55G11.2	–	–	10.4	2.9	–	–	rSKN-1, iIR	(Block et al., 2015; Engelmann et al., 2011; Evans et al., 2008; Oliveira et al., 2009; Troemel et al., 2006)
F56D5.3	–	–	3.1	1.8	–	–	rSKN-1, OxStrR	(Oliveira et al., 2009; Park et al., 2009)
H25K10.1	–	ACP7	1.9	–	–	–	rSKN-1, iIR, mib	(Engelmann et al., 2011; Oliveira et al., 2009; WormBase, 2021)
W06H8.2	–	–	4.9	4.4	–	–	rSKN-1	(Przybysz et al., 2009)
Y73B6BL.14	–	–	2.1	2.0	–	–	rSKN-1, DNArep	(Oliveira et al., 2009; WormBase, 2021)
ZK742.4	–	–	2.3	2.8	–	–	rSKN-1, rDAF-16	(McElwee et al., 2003; Oliveira et al., 2009)
R186.8	–	–	−1.8	–	–	–	T*l*R	(WormBase, 2021)
Y80D3A.2	*emb-4*	AQR	1.9	–	–	–	T*l*R	(WormBase, 2021)
Y48G10A.4	*ints-8*	INTS8	–	–	1.5	1.5	T*l*R	(WormBase, 2021)
D1007.12	*rpl-24.1*	RPL24	1.9	–	–	–	T*l*R	(WormBase, 2021)
Y92C3B.2	*uaf-1*	U2AF2	–	–	–	1.6	TlR	(WormBase, 2021)
Y53C12B.3	*nos-3*	–	–	−2.1	2.1	2.3	T*l*R, iIR	(O'Rourke et al., 2006; Pujol et al., 2008; WormBase, 2021)
F29C12.3	*rict-1*	RICTOR	–	–	1.8	–	TOR	(Blackwell et al., 2019; WormBase, 2021)
F56A3.5	*bro-1*	CBFB	–	−2.0	–	−2.8	TxR	(WormBase, 2021)
H25P06.2	*cdk-9*	CDK9	–	–	1.7	–	TxR, hhDG	(WormBase, 2021)
C16C2.1	*ceh-5*	NOTO, VAX1	–	−2.8	–	−1.8	TxR, hhDG	(WormBase, 2021)
ZK265.4	*ceh-8*	RAX	–	−3.1	–	–	TxR, hhDG	(WormBase, 2021)
C13G5.1	*ceh-16*	EN1, EN2	–	–	−1.8	–	TxR, hhDG	(WormBase, 2021)
C37E2.4	*ceh-36*	OTX1, OTX2	–	−2.1	–	–	TxR, hhDG	(WormBase, 2021)
ZK993.1	*ceh-45*	GSC	–	–	−2.2	–	TxR	(WormBase, 2021)
F34D6.2	*ceh-87*	ZHX1	−1.9	–	–	–	TxR	(WormBase, 2021)
T23D8.8	*cfi-1*	ARID3A, ARID3C	1.7	2.1	–	–	TxR	(WormBase, 2021)
F44B9.3	*cit-1.2*	CCNT1	–	–	1.8	–	TxR	(WormBase, 2021)
C15C8.2	*cky-1*	NPAS4	–	−2.1	–	–	TxR	(WormBase, 2021)
C34E10.7	*cnd-1*	NEUROD1	–	−2.4	–	–	TxR, hhDG	(WormBase, 2021)
F25E2.5	*daf-3*	SMAD4	–	−1.6	−2.4	−2.3	TxR, TGFβ, hhDG, mib	(WormBase, 2021)
C27C12.6	*dmd-4*	DMRT3	–	−1.8	–	–	TxR	(WormBase, 2021)
F54F7.7	*dot-1.2*	DOT1L	1.6	–	–	–	TxR, DNArep	(WormBase, 2021)
F49E12.6	*efl-3*	E2F7	–	−1.9	–	–	TxR	(WormBase, 2021)
C08C3.1	*egl-5*	HOXB8	–	–	−1.7	–	TxR	(WormBase, 2021)
F40H3.4	*fkh-8*	FOXR1	–	−2.7	–	−1.6	TxR	(WormBase, 2021)
C14B9.6	*gei-8*	NCOR1	1.7	–	–	–	TxR	(WormBase, 2021)
ZK131.3	*his-9*	–	–	–	–	−1.7	TxR	(WormBase, 2021)
ZK131.5	*his-11*	H2BC1	–	1.7	–	−1.6	TxR	(WormBase, 2021)
F38C2.2	*hlh-17*	BHLHE23	−1.7	−1.7	–	–	TxR	(WormBase, 2021)
T01D3.2	*hlh-34*	NPAS1	–	−3.7	–	−2.1	TxR, hhDG	(WormBase, 2021)
F43G6.6	*jmjd-1.1*	KDM7A	–	–	−2.1	–	TxR, hhDG, mib	(WormBase, 2021)
F23D12.5	*jmjd-3.2*	KDM6A, UTY	–	−1.7	–	–	TxR, hhDG	(WormBase, 2021)
F20H11.2	*let-765*	SBNO1	–	–	–	1.5	TxR	(WormBase, 2021)
T14F9.5	*lin-32*	ATOH1	–	−1.8	–	–	TxR, hhDG	(WormBase, 2021)
C01H6.5	*nhr-23*	RORC	1.8	–	–	–	TxR, hhDG	(WormBase, 2021)
C25E10.1	*nhr-30*	–	–	–	−2.5	–	TxR, mib	(WormBase, 2021)
F44C4.2	*nhr-37*	PPARA	–	–	–	−2.2	TxR, hhDG, mib	(WormBase, 2021)

Table 2 (*continued*)

sequence	gene name	human homolog(s)	NaAsO2	DMA	HgCl2	meHgCl	category	references
T09A12.4	*nhr-66*	–	–	–	1.5	–	TxR, mib	(WormBase, 2021)
H12C20.3	*nhr-68*	–	–	–	–	−1.7	TxR, mib	(WormBase, 2021)
C47F8.8	*nhr-81*	–	1.9	–	–	–	TxR, mib	(WormBase, 2021)
T13F3.3	*nhr-127*	PPARA	–	−4.0	–	−2.0	TxR, mib	(WormBase, 2021)
C03G6.8	*nhr-147*	HNF4A, HNF4G	–	−3.1	−2.0	−2.1	TxR, hhDG, mib	(WormBase, 2021)
C06B8.1	*nhr-150*	PPARA	–	−2.4	−1.8	−1.6	TxR, hhDG, mib	(WormBase, 2021)
C54F6.8	*nhr-171*	–	–	−2.4	−1.9	−1.8	TxR, mib	(WormBase, 2021)
F47C10.4	*nhr-187*	–	–	−2.3	−1.7	–	TxR, mib	(WormBase, 2021)
F47C10.7	*nhr-188*		–	–	−1.7	−1.7	TxR, mib	(WormBase, 2021)
R07B7.14	*nhr-207*	HNF4A, HNF4G	–	–	–	−1.6	TxR, hhDG, mib	(WormBase, 2021)
T07C5.3	*nhr-214*	–	–	−4.4	–	–	TxR	(WormBase, 2021)
T13F3.2	*nhr-218*	PPARA	–	−3.8	–	–	TxR, mib	(WormBase, 2021)
Y116A8C.18	*nhr-229*	–	–	–	–	−2.6	TxR, mib	(WormBase, 2021)
F21D12.5	*npax-1*	–	–	−1.7	−1.8	−1.8	TxR	(WormBase, 2021)
M6.3	*pha-2*	HHEX	−1.6	−1.9	–	−1.8	TxR	(WormBase, 2021)
F38A6.1	*pha-4*	FOXA1, FOXA2	−1.5	–	–	–	TxR	(WormBase, 2021)
C47C12.3	*ref-2*	ZIC1	–	−2.0	−1.7	–	TxR, hhDG	(WormBase, 2021)
F26A3.8	*rrf-1*	–	–	–	1.8	–	TxR	(WormBase, 2021)
T05A10.1	*sma-9*	HIVEP1	–	–	−1.6	–	TxR, TGFβ, hhDG	(WormBase, 2021)
Y43F4B.3	*set-25*	–	–	–	1.8	–	TxR, mib	(Klosin et al., 2017; WormBase, 2021)
W02H5.7	*sknr-1*	NFE2L1	–	–	−1.5	–	TxR, hhDG	(WormBase, 2021)
T08A11.2	*sftb-1*	SF3B1	–	–	1.7	–	TxR, hhDG	(WormBase, 2021)
F31E8.3	*tab-1*	BSX	−1.6	−2.6	−2.0	−1.7	TxR	(WormBase, 2021)
T07C4.2	*tbx-8*	EOMES, TBR1	–	–	−2.3	–	TxR, hhDG	(WormBase, 2021)
D2030.9	*wdr-23*	DCAF11	1.5	1.5	–	–	TxR	(WormBase, 2021)
ZC123.3	*zfh-2*	ZFHX3	–	–	1.5	–	Txr, hhDG	(WormBase, 2021)
Y48G8AL.10	*znf-236*	ZNF729, ZNF99	–	–	–	1.9	TxR, hhDG	(WormBase, 2021)
D1044.6	–	ZNF318	2.1	–	–	–	TxR	(WormBase, 2021)
F26A10.2	–	ZNF148	–	–	−2.3	–	TxR	(WormBase, 2021)
M03D4.4	–	ZNF653	–	−3.3	–	–	TxR	(WormBase, 2021)
R10E4.11	–	–	–	–	−1.6	–	TxR	(WormBase, 2021)
Y111B2A.10	–	ZNF689	–	−1.7	−2.4	−2.6	TxR	(WormBase, 2021)
Y53C10A.15	–	–	–	–	–	−2.2	TxR	(WormBase, 2021)
Y56A3A.28	–	–	–	–	−2.4	–	TxR	(WormBase, 2021)
Y57G11C.9	–	PPHLN1	–	–	−2.0	–	TxR	(WormBase, 2021)
C03A7.14	*abu-8*	–	–	−2.5	–	–	UPR	(WormBase, 2021)
T10B5.5	*cct-7*	CCT7	–	–	1.9	–	UPR, Loco	(WormBase, 2021)
ZK970.2	*clpp-1*	CLPP	−1.8	–	–	–	UPR, hhDG	(WormBase, 2021)
F38A5.13	*dnj-11*	DNAJC2	–	–	−2.0	–	UPR	(WormBase, 2021)
F39B2.10	*dnj-12*	DNAJA1, DNAJA4	–	–	1.6	–	UPR, mib	(WormBase, 2021)
ZK1193.5	*dve-1*	SATB2	–	–	−1.7	−1.6	UPR, TxR, hhdG	(WormBase, 2021)
T12D8.8	*hip-1*	ST13	–	−1.6	–	–	UPR	(WormBase, 2021)
T22A3.2	*hsp-12.1*	HSPB2	–	−2.0	–	–	UPR	(WormBase, 2021)
Y46H3A.2	*hsp-16.41*	CRYAB, HSPB6	–	–	−1.6	–	UPR, iIR, hhDG	(O'Rourke et al., 2006; Wong et al., 2007; WormBase, 2021)
T27E4.3	*hsp-16.48*	–	−1.5	–	–	–	UPR	(WormBase, 2021)
C15H9.6.3	*hsp-3*	HSPA5	–	–	1.7	–	UPR	(WormBase, 2021)
ZK256.1	*pmr-1*	ATP2C1	–	–	1.5	–	UPR, iIR, OxStrR, hhDG	(Kourtis et al., 2012; Schifano et al., 2019; WormBase, 2021)
T02C5.5	*unc-2*	CACNA1A	−1.5	–	–	–	UPR, TGFβ, hhDG, Loco, mib	(WormBase, 2021)
W01B6.1	*cwn-2*	WNT5A	–	−1.7	−1.6	–	Wnt, hhDG	(WormBase, 2021)
F58G4.4	*sdz-23*	–	−3.4	−2.6	−2.3	−2.7	rWnt	(Lezzerini and Budovskaya, 2014)

AMPK, effector of AMP-activated Protein Kinase Signaling; rAMPK, regulated by effectors of AMPK signaling; DAF-2/IIS, effector of the Insulin/Insulin-like Growth Factor Signaling Pathway; rDAF-16, regulated by DAF-16 in the same direction; DNArep, DNA replication/repair; DrugR, response to drug, xenobiotic metabolic process; hhDG, close homology to human disease gene(s); iIR, innate Immune Response (≥1.5x change in the same direction with exposure to ≥ two different pathogens or in ≥ two studies, or role in iIR described); Loco, involved in locomotion or behavior; MAPK, effector of Mitogen-Activated Protein Kinase Signaling (ERK, p38, JUK/SAPK); rMAPK, regulated by effectors of MAPK signaling; mib, metal ion binding; OxStrR, oxidative stress response; PCD, effector of programmed cell death and/or apoptotic process; rSKN-1, regulated by Nrf/SKN-1 in the same direction; TGFβ, effector of transforming growth factor beta receptor signaling pathway; TlR, Translational regulation and machinery; TOR, effector of TOR signaling; TxR, transcriptional regulation and/or histone modification; UPR, effector of unfolded protein/heat shock response; rUPR, regulated by UPR effectors; Wnt, effector of Wnt signaling; rWnt, regulated by Wnt signaling.

across all four tested conditions, there was a trend towards downregulation of transcriptional activators, and upregulation of negative regulators, consistent with a higher proportion of genes being downregulated for each chemical.

The GO terms "integral component of membrane" or "integral component of plasma membrane" (Membrane Bound) were associated with about 20% of upregulated DEGs for all four contidions. About 16% of DEGs downregulated by either form of mercury were in this

category. In contrast, 35% of genes downregulated by NaAsO2 and 26% of genes downregulated by DMA were known or predicted to encode membrane proteins.

One way to assess the specificity of response to a condition is to assess the proportion of DEGs that were also affected by other chemicals and the pathways those chemicals affect. 50–80% of DEGs affected by DMA were also affected by metformin, psoralens, rifampin, and sirolimus, drugs that influence energy production, mutagenesis, bacterial RNA synthesis, and inflammation, respectively (Fig. 3C). Sharing gene expression patterns with drugs that alter such a wide variety of processes is a likely indication of a generalized toxic response. In contrast to DMA, 31–62% of DEGs induced by NaAsO2 were also influenced by these same drugs, and this was the case for only 20–42% of DEGs for the two mercury compounds. By this measure, the specificity of toxic response would be ranked meHgCl = HgCl2 ≥ NaAsO2 > DMA.

3.2.3. Adult native gene expression – Curated genes

Genes with the greatest fold-change up or down in each set were further curated for references in the literature to clarify function. Only genes for which some functional or expression information could be identified were included in this count. These curated genes included 100 up and down DEGs from each condition, with the exception of HgCl2 and meHgCl which only had 87 and 52 informative upregulated DEGs respectively. Therefore, all upregulated genes for the two mercury compounds were included in the curated analysis. According to WormBase, 34 to 38 of the 100 DEGs most highly upregulated by NaAsO2 and DMA had human homologs, and about a third of these were human disease related. Given that *C. elegans* homologs have been identified for 60–80% of human genes (Kaletta and Hengartner, 2006), it was surprising that only about 20% of the 100 genes most highly downregulated by the two forms of arsenic had human homologs (Fig. 4A). HgCl2 upregulated DEGs had the highest proportion of human homologs at 69%, and over half of these human homologs, or 38% of all genes upregulated by HgCl2, were human disease related (Fig. 4B). For meHgCl upregulated genes, 36% had human homologs and two thirds of these were human disease related. Among highly downregulated genes with human homologs, meHgCl had the most at 33 of 100, and half of these were human disease related.

These curated genes were further evaluated in the literature for functional information. In Section 3.2.2 and in Fig. 3, all DEGs with an immune related GO term were included in the Innate Immune category. Here, for this curated set of high-fold-change genes, DEGs were instead put in an immune responder category (Immune Resp.) only if they were reported to be regulated in the same direction by at least 1.5-fold in response to two or more pathogens, or to a single pathogen in at least two studies, or to be required for immune defense (see Methods, Section 2.7). By this measure, 24 and 23 of the 100 highest fold change DEGs upregulated by NaAsO2 and DMA, respectively, are innate immune responders (Fig. 4A). In contrast, only 5–8% of DEGs upregulated by the two forms of mercury were immune responders (Fig. 4B).

Alternatively spliced isoforms of *skn-1* are orthologous to the mammalian transcription factors Nrf1 and Nrf2 (NF-E2-related factors), and Nrf/SKN-1 regulated pathways include oxidative stress response and immune function (Blackwell et al., 2019; Oliveira et al., 2009). Curated DEGs were categorized as Nrf/SKN-1 pathway responders if they had been reported to be regulated in the same direction by SKN-1. DEGs controlled by Nrf/SKN-1 made up 34% and 29% of the 100 genes most highly upregulated by NaAsO2 and DMA, respectively (Fig. 4A). Nrf/SKN-1 regulated DEGs highly induced by both NaAsO2 and DMA in the immune pathway responder category included *asp-14*, *dod-17*, *dod-24*, C32H11.3, C32H11.4, F01D5.3, and F55G11.2. Genes highly upregulated by both forms of arsenic that are in the oxidative stress responder category and known to be induced by Nrf/SKN-1 included *gcs-1*, *gst-10*, *gst-12*, *gst-13*, *gst-14*, *gst-16*, *gst-25*, *gst-30*, *gst-35*, and *gsto-2* (Table 2). Few Nrf/SKN-1 regulated genes were affected by exposure to the two mercury compounds at assessed concentrations (Fig. 4B). However, consistent with previous reports in *C. elegans* and mammals (Martinez-Finley et al., 2013a; Ruszkiewicz et al., 2018), *skn-1* itself was upregulated 1.5x by meHgCl (Table 2).

DAF-16 and SKN-1 are transcription factors for separate but interacting pathways that regulate stress resistance and immune defense, among other functions. Few curated DEGs for any condition were regulated by DAF-16 or its insulin/IGF-1 signaling (IIS) regulator DAF-2, indicating that IIS does not play a large role in the transcriptional response to arsenic or mercury at tested concentrations (Fig. 4). Similarly, few curated genes were found to be either effectors of, or downstream responders to, other pathways of toxicity such as epigenetic regulation, DNA damage response, the MAPK cascade, osmotic stress, lipid metabolism, or unfolded protein response (Supplemental Table 1).

3.3.1. Transgene expression – Oxidative stress response

Strains containing integrated GFP transgenes controlled by the promoters for *glutathione-S-transferase 4* (Leiers et al., 2003) (*gst-4*p::GFP, Fig. 5A-B) and gamma glutamylcysteine synthetase (*gcs-1*p::GFP), which catalyzes the first rate-limiting step of glutathione synthesis (An and Blackwell, 2003), were used to assess OxStrR in adult *C. elegans*. At concentrations relevant to developmental delay, NaAsO2 strongly induced both OxStrR reporters, while concentrations in the range of 20-fold higher DMA were required to induce similar levels of transgene induction (Fig. 5C-D). Concentrations of meHgCl above the developmental delay LOEL of 0.5 μg/ml induced both OxStrR biomarkers, while HgCl2 only induced *gst-4*p::GFP, and only at 5.0 μg/ml (Fig. 5E-F). At concentrations from 1.5 to 3.0 μg/ml, meHgCl induced slightly higher GFP fold changes than did NaAsO2 at the same concentrations, indicating a high OxStrR with meHgCl. At higher concentrations of HgCl2 there was a continued trend towards increased OxStrR with *gst-4*::GFP (data not shown), however changes in time-of-flight and extinction indicated that mercury had adversely affected *C. elegans* length and optical density, whole body morphology markers that reflect general health, making results less reliable.

3.3.2. Transgene expression – Unfolded protein response

Unfolded Protein Response (UPR) pathways are a key protective response for resisting the effects of some toxic agents. AIRAP/*aip-1* encodes an arsenite-inducible proteasome subunit required for resistance to arsenic toxicity in mammals and *C. elegans* (Sok et al., 2001; Stanhill et al., 2006). NaAsO2 induced *aip-1*p::GFP in a clear dose–response curve from 50 to 250 μg/ml (0.4–2 mM). In contrast to arsenite, DMA had no consistent effect on this proteasome specific UPR (UPR_{PS}) biomarker at any tested concentration (Fig. 6A).

C. elegans hsp-4 is a close homolog of the mammalian ER-localized Hsp70 chaperone BiP, and activation of the transgene *hsp-4*p::GFP is used as a biomarker of endoplasmic reticulum specific UPR (UPR_{ER}). UPR_{ER} is upregulated in response to ER stress and to tunicamycin, an inhibitor of N-linked glycosylation of nascent proteins (Bull and Thiede, 2012). Both forms of arsenic decreased expression of *hsp-4*p::GFP. NaAsO2 significantly decreased expression of this UPR_{ER} marker only at the highest assessed concentration of 150 μg/ml (1.15 mM), while expression was decreased in a dose response fashion with DMA from 25 to 250 μg/ml (180 μM to 1.8 mM) (Fig. 6B).

HgCl2 slightly but significantly increased UPR_{PS} at 3–4 μg/ml (11–15 μM) while meHgCl increased it only at the highest assessed concentration of 2.5 μg/ml (10 μM) (Fig. 6C). The UPR_{ER} marker induced opposite effects for HgCl2 and meHgCl, with HgCl2 increasing expression at 3–4 μg/ml (11–15 μM) and meHgCl decreasing expression between 0.5 and 3.0 μg/ml (2–12 μM) (Fig. 6D).

The two UPR biomarker strains used in this study took longer to grow from egg to egg-laying adult than wild type N2 *C. elegans* and had much lower reproductive outputs. Additionally, they were more

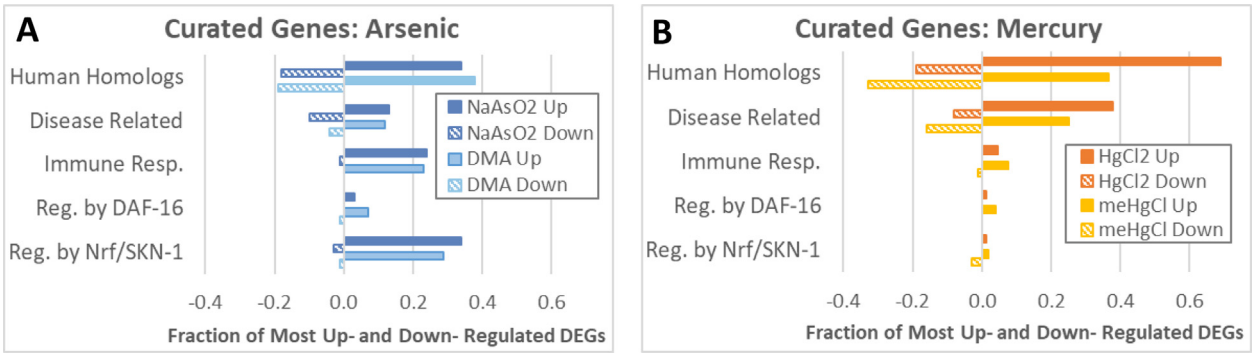

Fig. 4. Curation of DEGs with the greatest fold-change. (A-B) A subset of the most highly differentially regulated genes were further researched for functional information. Abbreviations: regulated (Reg.) in the same direction by DAF-16 or Nrf/SKN-1, genes that respond in the same direction to pathogen exposure (Immune Resp.).

sensitive to toxic stress from compounds tested here, as indicated by reduced TOF and EXT values (Supplemental Fig. 1B). Therefore, more care was required to accurately evaluate life stage for consistent dosing, and fewer concentrations could be assessed, limiting their value for higher-throughput toxicity analyses.

4. Discussion

Various forms of arsenic occur naturally in food and drinking water sources, but risk assessment and regulation are complicated by the fact that the toxicity of arsenic varies widely depending on its chemical composition (Benramdane et al., 1999; Feldmann and Krupp, 2011; Luvonga et al., 2020; Thomas et al., 2001). Many adverse effects of sodium arsenite (NaAsO2) are well understood, but there is little experimental data on the developmental toxicity of dimethylarsinic acid (DMA) (FDA, 2016). DMA has been found in some foods marketed to babies and children, and DMA was detected rodent pups whose dams had been exposed to arsenite in drinking water (FDA, 2016; Twaddle et al., 2018), indicating the importance of filling data gaps on the effects of oral exposure to DMA. In a large study of about 900 chemicals, *C. elegans* was nearly as good at predicting developmental toxicity in rats or rabbits as those two species were at predicting each other (Boyd et al., 2016). Additionally, the toxicodynamics and apical effects of many types of chemicals are similar in *C. elegans* and mammals, indicating that the *C. elegans* model has the potential to contribute useful information to human predictive integrated testing strategies (Hartman et al., 2021; Masjosthusmann et al., 2018; Parish et al., 2020).

With the worm Development and Activity Test (wDAT), the time for developing *C. elegans* to reach the third larval stage was used as a benchmark developmental milestone to assess the effects of organic and inorganic forms of arsenic and mercury. Across a range of concentrations, similar levels of developmental delay were associated with 20-fold higher concentrations of DMA relative to NaAsO2, with lowest observed effect levels (LOELs) at 10 μg/ml (76 μM) NaAsO2 or 200 μg/ml (1.4 mM) DMA (Fig. 1B). While the endpoint is different, this toxicity ratio is consistent with relative reported rat LD50s (Table 1).

Both the U.S. EPA's reference doses for oral exposure and the European Food Safety Authority's tolerable weekly intakes (Table 1) set limits for methylmercury exposure at about one third that of inorganic mercury based on the documented detrimental effects of methylmercury at low concentration on the developing nervous system (ATSDR, 1999; Davidson et al., 2004; EFSA, 2012; Tucker and Nowak, 2018). Methylmercury chloride (meHgCl) is also more toxic than mercury chloride (HgCl2) to developing *C. elegans* (Helmcke et al., 2009; McElwee and Freedman, 2011; Wyatt et al., 2016), though to our knowledge the relative toxicity of these two forms of mercury across a range of concentrations has not been established. Consistent with the difference in recommended safe exposures for humans, we found similar levels of developmental delay in *C. elegans* with 2 to 4-fold lower concentrations of meHgCl relative to HgCl2. The LOELs for developmental delay as assessed by the wDAT were 0.5 μg/ml (2 μM) for meHgCl and 2.0 μg/ml (7.5 μM) for HgCl2 (Fig. 1D).

While safe levels for oral exposure to inorganic arsenic (iAs) are a current matter of debate and experimental data on DMA in mammals is sparse, there is ample human epidemiologic evidence that robust metabolism of iAs to DMA is protective against arsenic toxicity (FDA, 2016; Schlebusch et al., 2015). In terms of human health it has been noted that, in general, methylation of inorganic species increases the toxicity of mercury but decreases the toxicity of arsenic (Francesconi, 2007), and this was also true in *C. elegans*, with a developmental toxicity ranking of meHgCl > HgCl2 > NaAsO2 ≫ DMA.

In developing mammals, the nervous system is one of the primary targets for both arsenic and mercury toxicity (Chandravanshi et al., 2018; Davidson et al., 2004), and altered motor activity is a frequently used measure of neurotoxicity (Aschner et al., 2017; Crofton et al., 1991; Mullenix, 1989). With inorganic HgCl2 and NaAsO2, there were low levels of hypoactivity at some concentrations in developing *C. elegans*, but consistent changes in population locomotor activity levels were not observed. For organic meHgCl and DMA however, there was a non-significant trend towards hyperactivity at below LOEL concentrations for developmental delay, and significant hypoactivity that increased with dose at concentrations above developmental delay LOELs (Fig. 1). Exposure to methylmercury during development has long been known to be associated with juvenile hypoactivity in mammals (Fredriksson et al., 1993; Schalock et al., 1981) and this effect was conserved in *C. elegans*. It is noteworthy that a. organic arsenicals are not known to be mammalian developmental neurotoxins while methylmercury is a known mammalian developmental neurotoxin, and b. in *C. elegans*, for meHgCl and DMA, the lowest concentrations at which significant developmental hypoactivity was observed differed by 300-fold. Therefore, it is possible that the exposure concentration at which changes in locomotor activity are observed during *C. elegans* development could be used to infer developmental neurotoxicity, however current data are insufficient to determine a range for this type of correlation.

For the purpose of identifying modes of toxic action that are specific to the test articles in question, it is important to avoid high concentrations that induce nonspecific toxicity and general cellular stress. Additionally, global gene expression assessment in *C. elegans* juveniles is complicated by the fact that expression levels of many genes fluctuate dramatically through the course of development, and therefore changes may be due to the developmental delay rather than directly due to the toxic agent. Therefore, LOEL concentrations for developmental delay in juveniles were utilized to assess gene expression

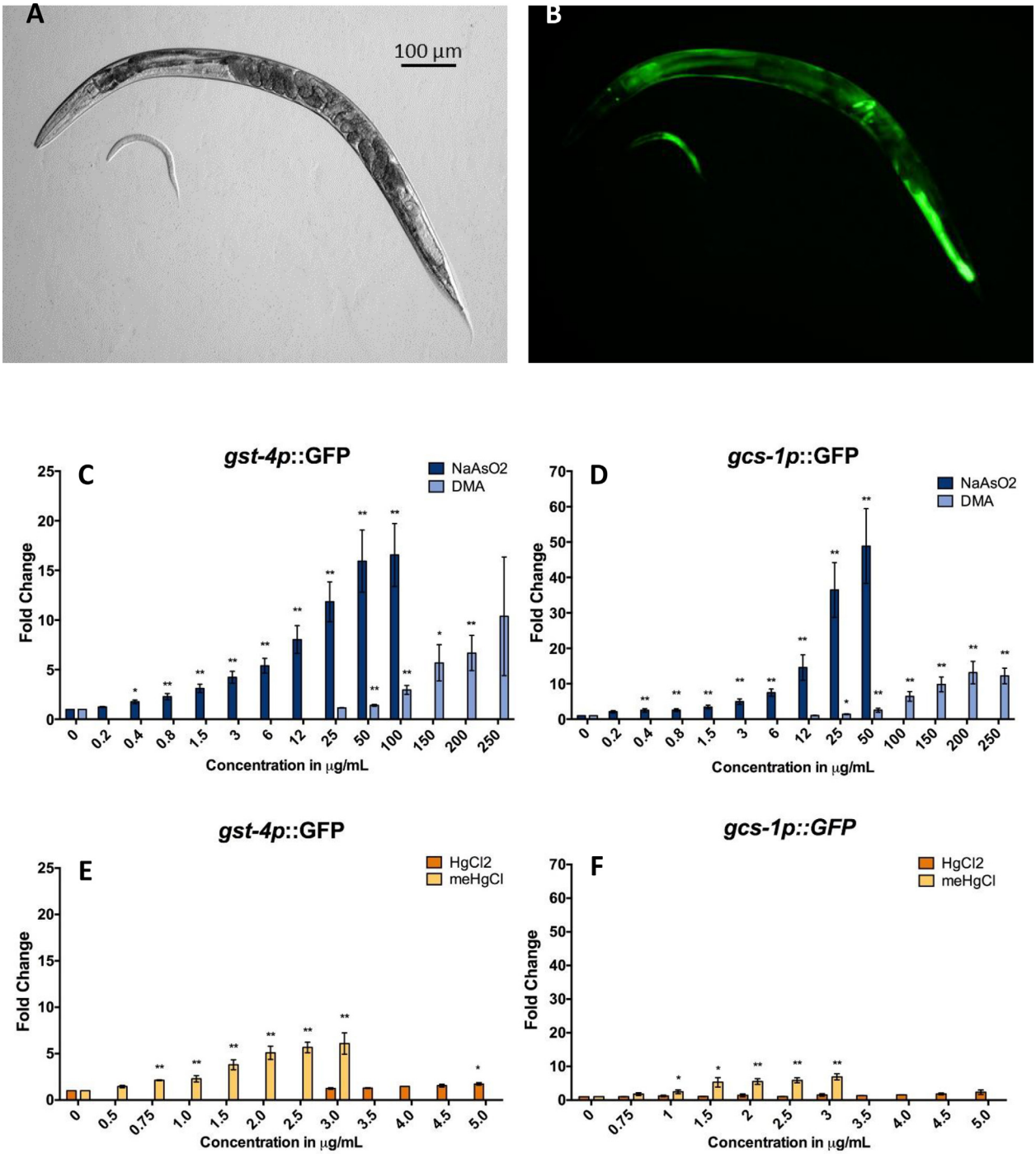

Fig. 5. Assessment of Oxidative Stress Response (OxStrR) Biomarkers. (A-B) Examples of bright field and fluorescence images of *C. elegans* carrying an integrated transgene with the promoter for phase II enzyme *gst-4* fused to GFP to monitor OxStrR. (C-F) Biosensor fold-change relative to water control, from at least three independent experiments per exposure group. Top concentrations shown are maximum concentration not altering adult size and optical density below 80% of control. Error bars: standard error of the mean (SEM), T-test p-values * < 0.05, ** < 0.005.

changes in adult *C. elegans* using gene expression microarrays. NaAsO2 at 10 µg/ml and DMA at 200 µg/ml induced 927 and 1,221 differentially expressed genes (DEGs), respectively (Fig. 2B). For DMA, that is an approximately 30% increase in the number of affected genes relative to NaAsO2 at a 20-fold higher DMA concentration. This is consistent with both relatively low developmental toxicity of DMA in *C. elegans*, and with human epidemiologic data correlating toxicity with consumption of iAs, but not with organic arsenic (ATSDR, 2007; Filippini et al., 2018; Hackethal et al., 2021). Only 161 of the DEGs induced by NaAsO2 or DMA were shared, however the patterns for GO terms were similar (Fig. 3A). Many of the DEGs that were induced by both arsenic compounds are involved in immune and oxidative stress responses, indicating that for these pathways their effects overlap, albeit at very different exposure levels.

2.0 µg/ml HgCl2 and 0.5 µg/ml meHgCl induced 670 and 485 DEGs, respectively. In contrast to arsenic, the GO term category patterns for the two mercury compounds varied considerably, consistent with differing effects. These results with synchronized adult cohorts

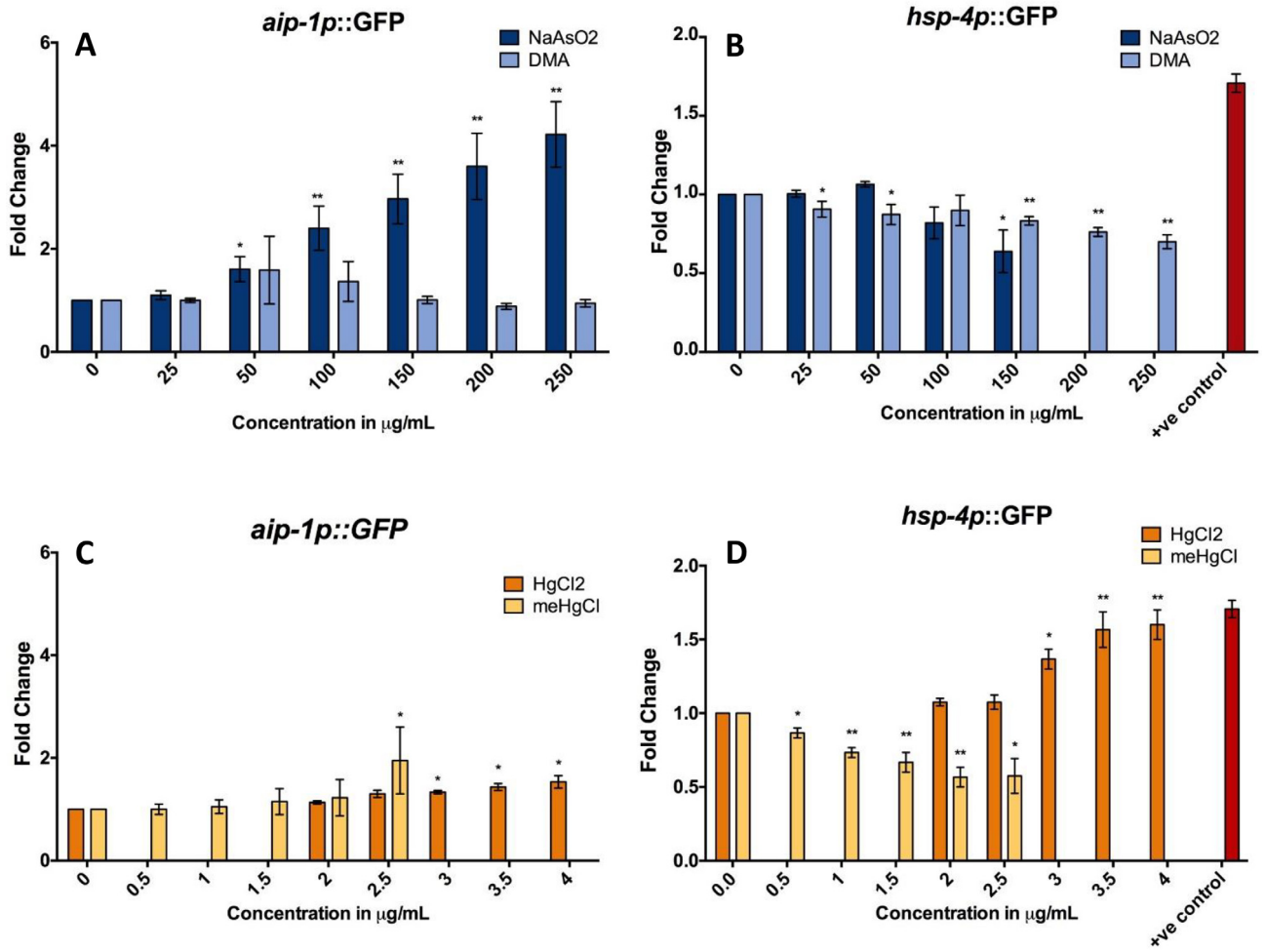

Fig. 6. Assessment of Unfolded Protein Response (UPR) Biomarkers. (A-D) UPR response biosensor fold change relative to water control, from at least three independent experiments per exposure group. (A&C) Proteasome specific UPR reporter *aip-1*p::GFP. (B&D) Endoplasmic reticulum specific UPR reporter *hsp-4*p::GFP (+ve control: 30 μg/ml Tunicamycin). Top concentrations shown are the maximum concentration not altering adult size or optical density below 80% of control. Error bars: standard error of the mean (SEM), T-test p-values * < 0.05, ** < 0.005.

are consistent with a previous report of disparate gene expression patterns with HgCl2 vs. meHgCl in human cell lines and in mixed population *C. elegans* (McElwee et al., 2013). While any chemical that adversely affects the development of an organism is considered a developmental toxin, the dose makes the poison. The relative number of DEGs induced in adults by concentrations that were equitoxic in juveniles can be an indicator of the specificity of a chemical's effects on developmental processes. The four compounds were tested in adults at concentrations that induced similar developmental delays in juveniles, yet the number of induced DEGs differed by 2.5-fold, with DMA inducing the most DEGs and meHgCl inducing the fewest. This likely reflects the specificity of methylmercury's developmental toxicity. Additionally, relative to the other compounds tested, a far higher proportion of genes influenced by DMA were also reported to be differentially regulated by a variety of chemicals and drugs with disparate cellular effects (Fig. 3C), consistent with DMA at high concentration inducing a more general form of toxicity relative to the other assessed conditions. Together, these results are consistent with greater mercury toxicity in juvenile mammals relative to adults and mercury's designation as a developmental toxin (WHO, 1991), and also suggest that the developmental delays and hypoactivity associated with high concentrations of DMA were likely related to more general modes of toxic action that are not specific to developmental processes.

Arsenic exposure affects mammalian immune function, with immune regulators and oxidative stress contributing to this mode of toxic action (Dangleben et al., 2013). Consistent with this, relative to the two mercury species, NaAsO2 and DMA induced changes in far more genes associated with glutathione, innate immune, and oxidation–reduction reaction related GO terms than did HgCl2 or meHgCl (Fig. 3A). In contrast, the proportion of both up- and downregulated genes with GO terms associated with nuclear localization and transcriptional regulation was higher for the two mercury species (Fig. 3B). While 21 DEGs encoding known or predicted transcription factors were regulated in the same direction by two or more tested conditions, the only histone modification related DEG shared was *his-11*, which was up with DMA but down with meHgCl, consistent with chemical specific modulation of genes related to histone modification. For all four compounds, there was a trend towards downregulation of genes involved with histone demethylation, and upregulation of histone methyltransferases. Overall, the direction of expression of genes involved in transcriptional regulation was towards condensation of chromatin and repression of transcription, potentially affecting biological processes including reproduction and transgenerational epigenetic regulation. Histone modification and reproductive toxicity assessment on exposed populations and their progeny will be conducted in a follow-up study to further evaluate these potential epigenetic effects.

Genes with the highest fold changes were further curated to identify trends or patterns. The proportion of the most highly upregulated genes with human homologs was greatest for HgCl2, and over half of

these are associated with human diseases (Fig. 4B). Many of the genes most highly regulated by HgCl2 exposure are associated with muscle and gait related diseases in humans including *clh-3* (CLCN2, myotonia congenita), *dyn-1* (DNM-1, Charcot-Marie-Tooth disease), *mup-2* (TNNT1, nemaline myopathy), *snf-6* (SLC6A14, Duchenne muscular dystrophy), and *unc-89* (SPEG, centronuclear myopathy). These changes in *C. elegans* are consistent with mammalian data linking mercury exposure to cardiomyopathies and neurological problems including tremors, paresthesia, weakness, slowed response, and unsteady gait (Ayensu and Tchounwou, 2006; Marsh et al., 1995; Myers et al., 1995; Prince and Rand, 2018). Relative to HgCl2, meHgCl affected fewer DEGs with homology to human disease genes, likely due to the four-fold lower tested concentration of methylmercury.

Conserved transcription factors Nrf1 and Nrf2, encoded in *C. elegans* as alternatively spliced isoforms of *skn-1*, are involved in regulating several pathways including those for metabolic and immune functions as well as oxidative stress resistance (Blackwell et al., 2019). Arsenite and methylmercury activate Nrf/SKN-1 in mammalian cell cultures and in *C. elegans* (Aono et al., 2003; Branco et al., 2014; Lau et al., 2013; Martinez-Finley et al., 2013b; Oliveira et al., 2009; VanDuyn et al., 2010). Genes known to be regulated by Nrf/SKN-1 were well represented among the curated DEGs most highly upregulated by NaAsO2 and DMA (Fig. 4A). *C. elegans* WDR-23 acts as a repressor for SKN-1, and *wdr-23* is activated by SKN-1 in a feed-back loop (Blackwell et al., 2015). Though it was not among the 100 most upregulated genes, *wdr-23* was upregulated 1.5-fold by both NaAsO2 and DMA (Table 2). Several genes known to be downregulated by SKN-1, including *clec-60*, *gst-19*, and *ins-7* (Miller et al., 2011; Oliveira et al., 2009), were also downregulated with both forms of arsenic. Together with innate immune and oxidative stress pathway responder genes being upregulated by both NaAsO2 and DMA at LOELs for developmental delay, these data suggest that Nrf/SKN-1 mediated activation of oxidative stress and innate immune response pathways are modes of toxic action for arsenic induced developmental delay.

At assessed concentrations, few curated DEGs affected by HgCl2 or meHgCl were found to be regulated by Nrf/SKN-1 (Fig. 4B). It is interesting to note however that in this study, only meHgCl upregulated expression of *skn-1* itself, which is consistent with previous findings that meHgCl upregulates *skn-1* and that Nrf/SKN-1 activity is essential for resistance to methylmercury toxicity in *C. elegans* and in mammalian cells (Branco et al., 2014; Martinez-Finley et al., 2013a; Martinez-Finley et al., 2013b; Toyama et al., 2007; VanDuyn et al., 2010).

C. elegans glutathione synthetase subunit *gcs-1* and glutathione-s-transferase *gst-4* are both direct targets of SKN-1, and transgenic strains with GFP expression controlled by the promoters for these two genes are used as biomarkers of Oxidative Stress Response (OxStrR) (Detienne et al., 2016). OxStrR is associated with mammalian exposures to organic and inorganic forms of mercury both *in vitro* and *in vivo* (Antunes Dos Santos (Antunes Dos Santos et al., 2018; Teixeira et al., 2018). In this study, microarray analysis of *C. elegans* gene expression at single, relatively low concentrations of the two mercury compounds did not induce genes associated with glutathione or oxidation–reduction processes (Fig. 3). Methylmercury concentrations above the 0.5 μg/ml tested with microarrays did activate both OxStrR reporters, however. In contrast, HgCl2 induced a significant increase in expression for only one of the two OxStrR reporters tested, and only at 5 μg/ml, the highest concentration that did not induce significant changes in adult length and optical density (Fig. 5). For arsenic, both OxStrR reporters were upregulated to a similar extent over a range of exposures by approximately 20-fold higher concentrations of DMA relative to NaAsO2 (Fig. 5). Interestingly, meHgCl at 1 to 3 μg/ml induced slightly higher expression levels with the two OxStrR reporters than did NaAsO2 at the same concentrations, consistent with methylmercury being an inducer of oxidative stress at low concentration. Together with developmental delay and microarray data, these results indicate that a. OxStrR biosensors can accurately reflect altered native gene expression, b. exposure to at least an order of magnitude more DMA is required relative to NaAsO2 for similar effects on multiple endpoints, c. for the two forms of arsenic, significant OxStrR was seen at LOEL concentrations for developmental delay, and d. as with mammals, biomarkers of OxStrR in *C. elegans* are associated with poor early developmental outcomes (Chandravanshi et al., 2018; Rains et al., 2021; Torres-Cuevas et al., 2017).

Unfolded Protein Response (UPR) pathways are activated with exposure to some chemicals and pathogen-produced toxins. Conserved arsenite-inducible proteasomal 19S regulatory particle-associated protein AIRAP/AIP-1 is involved in proteasome specific UPR (UPR_{PR}) and protects worms and mammalian cells from arsenite toxicity (Sok et al., 2001; Stanhill et al., 2006). As expected, NaAsO2 upregulated a UPR_{PR} reporter for AIRAP/AIP-1 expression in a strong dose response curve, but with a LOEL for UPR_{PR} induction in adults five times the NaAsO2 LOEL concentration for developmental delay. This is consistent with a previous report of DEGs associated with protein folding being induced in *C. elegans* exposed to NaAsO2 at 300 μg/ml but not at 30 μg/mL (Sahu et al., 2013). In contrast, DMA did not significantly upregulate this UPR_{PR} bioreporter at any concentration tested (Fig. 6A). HgCl2 and meHgCl increased expression of the transgenic UPR_{PR} reporter, but only slightly and also with LOELs for induction higher than LOELs for developmental delay.

Binding immunoglobulin protein (BiP) is a highly conserved molecular chaperone that acts in the endoplasmic reticulum (ER), and expression of the *C. elegans* BiP homolog *hsp-4* is used as a biomarker of ER specific UPR (UPR_{ER}) (Kapulkin et al., 2005). Under normal conditions, BiP/HSP-4 is closely regulated to align the folding capacity of the endoplasmic reticulum to the level of unfolded proteins present (Calfon et al., 2002; Taylor and Dillin, 2013). In contrast, UPR_{ER} is downregulated during aging, in response to certain chemicals, and in some disease states (Katayama et al., 1999; Naidoo et al., 2018; Tan et al., 2015; Yamagishi et al., 2012). Additionally, knockdown of BiP and decreased UPR_{ER} inhibits some viral infections, indicating that downregulation of UPR can be an effective immune response (Goodwin et al., 2011; Limjindaporn et al., 2009). The UPR_{ER} biomarker under the control of the *hsp-4* promoter was slightly but significantly downregulated by both meHgCl and DMA at LOEL concentrations for developmental delay. NaAsO2 also downregulated UPR_{ER}, but only at 150 μg/ml, a concentration far above those needed to induce developmental delay. In contrast to UPR_{ER} downregulation by meHgCl, HgCl2 upregulated the UPR_{ER} biomarker at concentrations relevant to developmental toxicity. These results further highlight the distinct stress responses to different chemical species of the same toxic elements.

Current data do not support the use of *C. elegans* toxicity responses alone to predict safe exposure levels in other species, however this work does suggest a preliminary ranking scheme. If toxicity in *C. elegans* were categorized as very toxic for responses at <5 μg/ml, toxic for 5 to 20 μg/ml, moderate toxicity for 20 to 100 μg/ml, and low toxicity for 100 μg/ml to 1 mg/ml, then for developmental toxicity both meHgCl and HgCl2 would be categorized as very toxic, NaAsO2 as toxic, and DMA as low toxicity. For oxidative stress, the categories would be slightly different, with NaAsO2 and meHgCl in the very toxic category, HgCl2 in the toxic category, and DMA in the moderate toxicity category.

In vertebrates, arsenite-3-methyltransferase (AS3MT) is considered by many to be the primary enzyme that methylates iAs to form organic metabolites, though there is growing evidence of other genes playing a significant role as well (Zdraljevic et al., 2019). While the *C. elegans* genome encodes homologs to the majority of human genes, it lacks a close AS3MT homolog (Cartwright, 2016). N-6-adenine-specific DNA methyltransferase 1 (N6AMT1) has been found to methylate arsenite *in vitro*, and polymorphisms of N6AMT1 are associated with changes

in arsenic metabolism in humans (Chen et al., 2017; Harari et al., 2013). The *C. elegans* gene *mtq-2* (MethylTransferase modifying glutamine (Q)) is a BLASTP match for N6AMT1 for 85.5% of length. Additionally, a search of Wormbase.org (Version: WS280) for methyltransferase genes in *C. elegans* yields nearly two hundred entries, so it is possible that one or more of these gene products can methylate iAs. If *C. elegans* do not methylate NaAsO2, then they model the toxicity of iAs without methylated metabolites. If *C. elegans* do methylate iAs, then they are a closer model to mammalian arsenic metabolism. This question will be answered with a follow-up study where we will assess arsenic uptake and speciation in *C. elegans*, as well as reproductive and germline toxicities.

5. Conclusions

Developmental toxicity was ranked meHgCl > HgCl2 > NaAsO2 ≈ DMA in *C. elegans*. In contrast, oxidative stress response was ranked NaAsO2 = meHgCl > HgCl2 > DMA in *C. elegans* adults. Relative to NaAsO2, exposures to approximately 20-fold higher concentrations of DMA induced similar levels of both developmental delay and oxidative stress. A bioreporter for conserved proteasome specific unfolded protein response (UPR_{PR}) was strongly induced by NaAsO2 but was not significantly altered by DMA, consistent with disparate effects on UPR_{PR} for these two forms of arsenic. Transgene expression of a conserved marker for ER specific unfolded protein response (UPR_{ER}) was increased by HgCl2 but decreased by meHgCl, consistent with disparate effects on UPR_{ER} for these two forms of mercury. As in juvenile rodents, *C. elegans* developmental exposure to meHgCl induced hypoactivity, indicating conservation of toxic effect. For both developmental toxicity and oxidative stress response in *C. elegans*, monomethylation increased mercury toxicity while dimethylation decreased arsenic toxicity. Transgene expression correlated well with native gene expression, indicating that fluorescence assessment using *C. elegans* GFP transgenic strains can accurately reflect pathway activation, however optimization of some strains would be required prior to use in higher-throughput analyses. Our findings in *C. elegans* reflect findings in mammals for which there is data, stress the disparity of effects from exposure to different chemical forms of arsenic and mercury, and indicate low oral toxicity for DMA relative to inorganic arsenic in this model organism.

Funding

All authors are FDA employees. This work was funded and conducted within the context of regular operating budgets and employment duties.

Declaration of Competing Interest

The authors declare that they have no known competing financial interests or personal relationships that could have appeared to influence the work reported in this paper.

Appendix A. Supplementary data

Supplementary data to this article can be found online at https://doi.org/10.1016/j.crtox.2022.100071.

References

Agger, K., Cloos, P.A.C., Christensen, J., Pasini, D., Rose, S., Rappsilber, J., Issaeva, I., Canaani, E., Salcini, A.E., Helin, K., 2007. UTX and JMJD3 are histone H3K27 demethylases involved in HOX gene regulation and development. Nature 449, 731–734. https://doi.org/10.1038/nature06145.

Aguado, A., Galan, M., Zhenyukh, O., Wiggers, G.A., Roque, F.R., Redondo, S., Pecanha, F., Martin, A., Fortuno, A., Cachofeiro, V., Tejerina, T., Salaices, M., Briones, A.M., 2013. Mercury induces proliferation and reduces cell size in vascular smooth muscle cells through MAPK, oxidative stress and cyclooxygenase-2 pathways. Toxicol. Appl. Pharmacol. 268, 188–200. https://doi.org/10.1016/j.taap.2013.01.030.

Almendinger, J., K. Doukoumetzidis, J.M. Kinchen, A. Kaech, K.S. Ravichandran, and M. O. Hengartner, 2011. A conserved role for SNX9-family members in the regulation of phagosome maturation during engulfment of apoptotic cells. PLoS One. 6: e18325. https://doi.org/10.1371/journal.pone.0018325.

An, J.H., Blackwell, T.K., 2003. SKN-1 links *C. elegans* mesendodermal specification to a conserved oxidative stress response. Genes Dev. 17, 1882–1893. https://doi.org/10.1101/gad.1107803.

Andersen, E.C., Horvitz, H.R., 2007. Two C. elegans histone methyltransferases repress lin-3EGF transcription to inhibit vulval development. Development. 134, 2991–2999. https://doi.org/10.1242/dev.009373.

Antunes dos Santos, A., Ferrer, B., Marques Gonçalves, F., Tsatsakis, A., Renieri, E., Skalny, A., Farina, M., Rocha, J., Aschner, M., 2018. Oxidative Stress in Methylmercury-Induced Cell Toxicity. Toxics. 6 (3), 47.

Aono, J., Yanagawa, T., Itoh, K., Li, B., Yoshida, H., Kumagai, Y., Yamamoto, M., Ishii, T., 2003. Activation of Nrf2 and accumulation of ubiquitinated A170 by arsenic in osteoblasts. Biochem. Biophys. Res. Commun. 305, 271–277. https://doi.org/10.1016/s0006-291x(03)00728-9.

Aschner, M., Ceccatelli, S., Daneshian, M., Fritsche, E., Hasiwa, N., Hartung, T., Hogberg, H.T., Leist, M., Li, A., Mundi, W.R., Padilla, S., Piersma, A.H., Bal-Price, A., Seiler, A., Westerink, R.H., Zimmer, B., Lein, P.J., 2017. Reference compounds for alternative test methods to indicate developmental neurotoxicity (DNT) potential of chemicals: example lists and criteria for their selection and use. ALTEX. 34, 49–74 https://doi.org/10.14573/altex.1604201.

Atsdr, 1999. Toxicological Profile for Mercury. U.S, Agency for Toxic Substances and Disease Registry. https://permanent.access.gpo.gov/gpo31588/tp46.pdf.

Atsdr, 2007. Toxicological Profile for Arsenic. U.S, Agency for Toxic Substances and Disease Registry. https://www.atsdr.cdc.gov/toxprofiles/tp2.pdf.

ATSDR. 2019. Substance Priority List. https://www.atsdr.cdc.gov/spl/index.html#2019spl.

Avila, A.M., Bebenek, I., Bonzo, J.A., Bourcier, T., Davis Bruno, K.L., Carlson, D.B., Dubinion, J., Elayan, I., Harrouk, W., Lee, S.L., Mendrick, D.L., Merrill, J.C., Peretz, J., Place, E., Saulnier, M., Wange, R.L., Yao, J., Zhao, D., Brown, P.C., 2020. An FDA/CDER perspective on nonclinical testing strategies: Classical toxicology approaches and new approach methodologies (NAMs). Regul. Toxicol. Pharm. 114,. https://doi.org/10.1016/j.yrtph.2020.104662 104662.

Ayensu, W.K., Tchounwou, P.B., 2006. Microarray analysis of mercury-induced changes in gene expression in human liver carcinoma (HepG2) cells: importance in immune responses. Int. J. Environ. Res. Public Health 3, 141–173. https://doi.org/10.3390/ijerph2006030018.

Benjamini, Y., Hochberg, Y., 1995. Controlling the False Discovery Rate: A Practical and Powerful Approach to Multiple Testing. J. Roy. Stat. Soc.: Ser. B (Methodol.) 57, 289–300. https://doi.org/10.1111/j.2517-6161.1995.tb02031.x.

Benramdane, L., Bressolle, F., Vallon, J.J., 1999. Arsenic speciation in humans and food products: a review. J. Chromatogr. Sci. 37, 330–344. https://doi.org/10.1093/chromsci/37.9.330.

Blackwell, T.K., Sewell, A.K., Wu, Z., Han, M., 2019. TOR Signaling in Caenorhabditis elegans Development, Metabolism, and Aging. Genetics 213, 329–360. https://doi.org/10.1534/genetics.119.302504.

Blackwell, T.K., Steinbaugh, M.J., Hourihan, J.M., Ewald, C.Y., Isik, M., 2015. SKN-1/Nrf, stress responses, and aging in Caenorhabditis elegans. Free Radic Biol Med. 88, 290–301. https://doi.org/10.1016/j.freeradbiomed.2015.06.008.

Block, D.H.S., Twumasi-Boateng, K., Kang, H.S., Carlisle, J.A., Hanganu, A., Lai, T.-J., Shapira, M., Tan, M.-W., 2015. The Developmental Intestinal Regulator ELT-2 Controls p38-Dependent Immune Responses in Adult C. elegans. PLoS Genet. 11 (5), e1005265.

Bolz, D.D., Tenor, J.L., Aballay, A., 2010. A conserved PMK-1/p38 MAPK is required in caenorhabditis elegans tissue-specific immune response to Yersinia pestis infection. J. Biol. Chem. 285, 10832–10840. https://doi.org/10.1074/jbc.M109.091629.

Boyd, W.A., McBride, S.J., Rice, J.R., Snyder, D.W., Freedman, J.H., 2010. A high-throughput method for assessing chemical toxicity using a *Caenorhabditis elegans* reproduction assay. Toxicol. Appl. Pharmacol. 245, 153–159. https://doi.org/10.1016/j.taap.2010.02.014.

Boyd, W.A., Smith, M.V., Co, C.A., Pirone, J.R., Rice, J.R., Shockley, K.R., Freedman, J. H., 2016. Developmental Effects of the ToxCast Phase I and Phase II Chemicals in *Caenorhabditis elegans* and Corresponding Responses in Zebrafish, Rats, and Rabbits. Environ. Health Perspect. 124, 586–593. https://doi.org/10.1289/ehp.1409645.

Branco, V., Godinho-Santos, A., Goncalves, J., Lu, J., Holmgren, A., Carvalho, C., 2014. Mitochondrial thioredoxin reductase inhibition, selenium status, and Nrf-2 activation are determinant factors modulating the toxicity of mercury compounds. Free Radic Biol Med. 73, 95–105. https://doi.org/10.1016/j.freeradbiomed.2014.04.030.

Bull, V.H., Thiede, B., 2012. Proteome analysis of tunicamycin-induced ER stress. Electrophoresis 33, 1814–1823. https://doi.org/10.1002/elps.201100565.

Calfon, M., Zeng, H., Urano, F., Till, J.H., Hubbard, S.R., Harding, H.P., Clark, S.G., Ron, D., 2002. IRE1 couples endoplasmic reticulum load to secretory capacity by processing the XBP-1 mRNA. Nature 415, 92–96. https://doi.org/10.1038/415092a.

Cartwright, I.L. 2016. Invertebrate Models in Arsenic Research: Past, Present, and Future. *In* Arsenic: Exposure Sources, Health Risks, and Mechanisms of Toxicity. J.C. States, editor. John Wiley & Sons, Inc. 469-493.

Cecere, G., Hoersch, S., Jensen, M.B., Dixit, S., Grishok, A., 2013. The ZFP-1(AF10)/DOT-1 Complex Opposes H2B Ubiquitination to Reduce Pol II Transcription. Mol. Cell 50, 894–907 https://doi.org/10.1016/j.molcel.2013.06.002.

Cfsan, 2015. 2015–2018 Science and Research Strategic Plan. U.S, Food and Drug Administration. https://www.fda.gov/Food/FoodScienceResearch/ResearchStrategicPlan/default.htm.
Chandravanshi, L.P., Gupta, R., Shukla, R.K., 2018. Developmental Neurotoxicity of Arsenic: Involvement of Oxidative Stress and Mitochondrial Functions. Biol. Trace Elem. Res. 186, 185–198. https://doi.org/10.1007/s12011-018-1286-1.
Chen, X., Guo, X., He, P., Nie, J., Yan, X., Zhu, J., Zhang, L., Mao, G., Wu, H., Liu, Z., Aga, D., Xu, P., Smith, M., Ren, X., 2017. Interactive Influence of N6AMT1 and As3MT Genetic Variations on Arsenic Metabolism in the Population of Inner Mongolia. China. Toxicol Sci. 155, 124–134. https://doi.org/10.1093/toxsci/kfw181.
Clegg, E.D., H.F. Lapenotiere, D.Y. French, and M. Szilagyi. 2002. Use of CeHR axenic medium for exposure and gene expression studies. *In* 2002 East Coast Worm Meeting, Reproductive Hazards Laboratory, US Army Center for Environmental Health Research, Fort Detrick, MD.
Congress, U.S., 2021. Baby Foods Are Tainted with Dangerous Levels of Arsenic, Lead, Cadmium, and Mercury. C.o.O.a.R. Subcommittee on Economic and Consumer Policy U.S, House of Representatives. https://www.eenews.net/assets/2021/02/04/document_gw_03.pdf.
Crofton, K.M., Howard, J.L., Moser, V.C., Gill, M.W., Reiter, L.W., Tilson, H.A., MacPhail, R.C., 1991. Interlaboratory comparison of motor activity experiments: implications for neurotoxicological assessments. Neurotoxicol. Teratol. 13, 599–609. https://doi.org/10.1016/0892-0362(91)90043-v.
Cui, Y., McBride, S.J., Boyd, W.A., Alper, S., Freedman, J.H., 2007. Toxicogenomic analysis of Caenorhabditis elegans reveals novel genes and pathways involved in the resistance to cadmium toxicity. Genome Biol. 8, R122. https://doi.org/10.1186/gb-2007-8-6-r122.
Dangleben, N.L., Skibola, C.F., Smith, M.T., 2013. Arsenic immunotoxicity: a review. Environ Health. 12, 73. https://doi.org/10.1186/1476-069X-12-73.
Davidson, P.W., Myers, G.J., Weiss, B., 2004. Mercury exposure and child development outcomes. Pediatrics 113, 1023–1029.
Del Razo, L.M., Quintanilla-Vega, B., Brambila-Colombres, E., Calderon-Aranda, E.S., Manno, M., Albores, A., 2001. Stress proteins induced by arsenic. Toxicol. Appl. Pharmacol. 177, 132–148. https://doi.org/10.1006/taap.2001.9291.
Detienne, G., Van de Walle, P., De Haes, W., Schoofs, L., Temmerman, L., 2016. SKN-1-independent transcriptional activation of glutathione S-transferase 4 (GST-4) by EGF signaling. Worm. 5,. https://doi.org/10.1080/21624054.2016.1230585 e1230585.
EFSA. 2009. EFSA Panel on Contaminants in the Food Chain (CONTAM): Scientific Opinion on Arsenic in Food. European Food Safety Authority (EFSA).
Efsa, 2012. Scientific Opinion on the risk for public health related to the presence of mercury and methylmercury in food. European Food Safety Authority https://efsa.onlinelibrary.wiley.com/doi/abs/10.2903/j.efsa.2012.2985.
Engelmann, I., Griffon, A., Tichit, L., Montañana-Sanchis, F., Wang, G., Reinke, V., Waterston, R.H., Hillier, L.W., Ewbank, J.J., Lehner, B., 2011. A comprehensive analysis of gene expression changes provoked by bacterial and fungal infection in *C. elegans*. PLoS ONE 6 (5), e19055.
Escudero-Lourdes, C., 2016. Toxicity mechanisms of arsenic that are shared with neurodegenerative diseases and cognitive impairment: Role of oxidative stress and inflammatory responses. Neurotoxicology. 53, 223–235. https://doi.org/10.1016/j.neuro.2016.02.002.
Evans, E.A., T. Kawli, and M.W. Tan, 2008. Pseudomonas aeruginosa suppresses host immunity by activating the DAF-2 insulin-like signaling pathway in Caenorhabditis elegans. PLoS Pathog. 4:e1000175. https://doi.org/10.1371/journal.ppat.1000175.
Fang, H., S.C. Harris, Z. Su, M. Chen, F. Qian, L. Shi, R. Perkins, and W. Tong. 2017. ArrayTrack: An FDA and Public Genomic Tool. *In* Biological Networks and Pathway Analysis. Vol. Methods in Molecular Biology. T. T. and N. Y., editors. Humana Press, New York, NY.
Faoun, who., 2011. Evaluation of Certain Contaminants in Food: Seventy-second report of the Joint FAO/WHO Expert Committee on Food Additives. World Health. Organization https://apps.who.int/iris/handle/10665/44520.
FDA, U.S. 2016. Arsenic in Rice and Rice Products Risk Assessment Report. Center for Food Safety and Applied Nutrition https://www.fda.gov/files/food/published/Arsenic-in-Rice-and-Rice-Products-Risk-Assessment-Report-PDF.pdf.
FDA, U.S. 2017. FDA's Predictive Toxicology Roadmap. https://www.fda.gov/ScienceResearch/AboutScienceResearchatFDA/ucm601090.htm.
FDA, U.S. 2020. Metals and Your Food. https://www.fda.gov/food/chemicals-metals-pesticides-food/metals-and-your-food.
FDA, u.s., 2021. Closer to Zero: Action Plan for Baby Foods. U.S, Food and Drug Administration. https://www.fda.gov/food/metals-and-your-food/closer-zero-action-plan-baby-foods.
Feldmann, J., Krupp, E.M., 2011. Critical review or scientific opinion paper: arsenosugars–a class of benign arsenic species or justification for developing partly speciated arsenic fractionation in foodstuffs? Anal. Bioanal. Chem. 399, 1735–1741. https://doi.org/10.1007/s00216-010-4303-6.
Filippini, T., Malavolti, M., Cilloni, S., Wise, L.A., Violi, F., Malagoli, C., Vescovi, L., Vinceti, M., 2018. Intake of arsenic and mercury from fish and seafood in a Northern Italy community. Food Chem. Toxicol. 116, 20–26. https://doi.org/10.1016/j.fct.2018.04.010.
Foster, K.J., Cheesman, H.K., Liu, P., Peterson, N.D., Anderson, S.M., Pukkila-Worley, R., 2020. Innate Immunity in the C. elegans Intestine Is Programmed by a Neuronal Regulator of AWC Olfactory Neuron Development. Cell Rep. 31 (107478). https://doi.org/10.1016/j.celrep.2020.03.042.
Francesconi, K.A., 2007. Toxic metal species and food regulations–making a healthy choice. Analyst. 132, 17–20. https://doi.org/10.1039/b610544k.
Fredriksson, A., Gardlund, A.T., Bergman, K., Oskarsson, A., Ohlin, B., Danielsson, B., Archer, T., 1993. Effects of maternal dietary supplementation with selenite on the postnatal development of rat offspring exposed to methyl mercury in utero. Pharmacol. Toxicol. 72, 377–382.
Gonzalez-Cabo, P., Bolinches-Amoros, A., Cabello, J., Ros, S., Moreno, S., Baylis, H.A., Palau, F., Vazquez-Manrique, R.P., 2011. Disruption of the ATP-binding cassette B7 (ABTM-1/ABCB7) induces oxidative stress and premature cell death in Caenorhabditis elegans. J. Biol. Chem. 286, 21304–21314. https://doi.org/10.1074/jbc.M110.211201.
Goodwin, E.C., A. Lipovsky, T. Inoue, T.G. Magaldi, A.P. Edwards, K.E. Van Goor, A.W. Paton, J.C. Paton, W.J. Atwood, B. Tsai, and D. DiMaio, 2011. BiP and multiple DNAJ molecular chaperones in the endoplasmic reticulum are required for efficient simian virus 40 infection. mBio. 2:e00101-00111. https://doi.org/10.1128/mBio.00101-11
Hackethal, C., Kopp, J.F., Sarvan, I., Schwerdtle, T., Lindtner, O., 2021. Total arsenic and water-soluble arsenic species in foods of the first German total diet study (BfR MEAL Study). Food Chem. 346,. https://doi.org/10.1016/j.foodchem.2020.128913 128913.
Hao, C., Hao, W., Wei, X., Xing, L., Jiang, J., Shang, L., 2009. The role of MAPK in the biphasic dose-response phenomenon induced by cadmium and mercury in HEK293 cells. Toxicol. In Vitro 23, 660–666. https://doi.org/10.1016/j.tiv.2009.03.005.
Harari, F., Engstrom, K., Concha, G., Colque, G., Vahter, M., Broberg, K., 2013. N-6-adenine-specific DNA methyltransferase 1 (N6AMT1) polymorphisms and arsenic methylation in Andean women. Environ. Health Perspect. 121, 797–803. https://doi.org/10.1289/ehp.1206003.
Hartman, J.H., Widmayer, S.J., Bergemann, C.M., King, D.E., Morton, K.S., Romersi, R.F., Jameson, L.E., Leung, M.C.K., Andersen, E.C., Taubert, S., Meyer, J.N., 2021. Xenobiotic metabolism and transport in Caenorhabditis elegans. J. Toxicol. Environ Health B Crit. Rev. 24, 51–94. https://doi.org/10.1080/10937404.2021.1884921.
Hasegawa, K., Miwa, S., Isomura, K., Tsutsumiuchi, K., Taniguchi, H., Miwa, J., 2008. Acrylamide-responsive genes in the nematode Caenorhabditis elegans. Toxicol. Sci. 101, 215–225. https://doi.org/10.1093/toxsci/kfm276.
Hasegawa, K., Miwa, S., Tsutsumiuchi, K., Miwa, J., Dalmasso, G., 2010. Allyl isothiocyanate that induces GST and UGT expression confers oxidative stress resistance on C. elegans, as demonstrated by nematode biosensor. PLoS ONE 5 (2), e9267.
Haskins, K.A., Russell, J.F., Gaddis, N., Dressman, H.K., Aballay, A., 2008. Unfolded protein response genes regulated by CED-1 are required for Caenorhabditis elegans innate immunity. Dev. Cell 15, 87–97. https://doi.org/10.1016/j.devcel.2008.05.006.
Helmcke, K.J., Syversen, T., Miller 3rd, D.M., Aschner, M., 2009. Characterization of the effects of methylmercury on *Caenorhabditis elegans*. Toxicol. Appl. Pharmacol. 240, 265–272. https://doi.org/10.1016/j.taap.2009.03.013.
Hillier, L.W., Coulson, A., Murray, J.I., Bao, Z., Sulston, J.E., Waterston, R.H., 2005. Genomics in C. elegans: so many genes, such a little worm. Genome Res. 15, 1651–1660. https://doi.org/10.1101/gr.3729105.
van der Hoeven, R., McCallum, K.C., Cruz, M.R., Garsin, D.A., Ausubel, F.M., 2011. Ce-Duox1/BLI-3 generated reactive oxygen species trigger protective SKN-1 activity via p38 MAPK signaling during infection in C. elegans. PLoS Pathog. 7 (12), e1002453.
Hou, N.S., Gutschmidt, A., Choi, D.Y., Pather, K., Shi, X., Watts, J.L., Hoppe, T., Taubert, S., 2014. Activation of the endoplasmic reticulum unfolded protein response by lipid disequilibrium without disturbed proteostasis in vivo. Proc Natl Acad Sci U S A. 111, E2271–2280. https://doi.org/10.1073/pnas.1318262111.
Huang da, W., Sherman, B.T., Lempicki, R.A., 2009. Bioinformatics enrichment tools: paths toward the comprehensive functional analysis of large gene lists. Nucleic Acids Res. 37, 1–13. https://doi.org/10.1093/nar/gkn923.
Hunt, P.R., 2017. The C. elegans model in toxicity testing. J. Appl. Toxicol. 37, 50–59. https://doi.org/10.1002/jat.3357.
Hunt, P.R., Camacho, J.A., Sprando, R.L., 2020. *Caenorhabditis elegans* for predictive toxicology. Current Opinion in Toxicology. 23–24, 23–28. https://doi.org/10.1016/j.cotox.2020.02.004.
Hunt, P.R., Olejnik, N., Bailey, K.D., Vaught, C.A., Sprando, R.L., 2018. C. elegans Development and Activity Test detects mammalian developmental neurotoxins. Food Chem. Toxicol. 121, 583–592. https://doi.org/10.1016/j.fct.2018.09.061.
Hunt, P.R., Olejnik, N., Sprando, R.L., 2012. Toxicity ranking of heavy metals with screening method using adult Caenorhabditis elegans and propidium iodide replicates toxicity ranking in rat. Food Chem. Toxicol. 50, 3280–3290. https://doi.org/10.1016/j.fct.2012.06.051.
Inoue, H., Hisamoto, N., An, J.H., Oliveira, R.P., Nishida, E., Blackwell, T.K., Matsumoto, K., 2005. The C. elegans p38 MAPK pathway regulates nuclear localization of the transcription factor SKN-1 in oxidative stress response. Genes Dev. 19, 2278–2283. https://doi.org/10.1101/gad.1324805.
Irazoqui, J.E., Troemel, E.R., Feinbaum, R.L., Luhachack, L.G., Cezairliyan, B.O., Ausubel, F.M., Guttman, D.S., 2010. Distinct pathogenesis and host responses during infection of *C. elegans* by P. aeruginosa and S. aureus. PLoS Pathog. 6 (7), e1000982.
IRIS. 1991. Chemical Risk Assessment Summary: Inorganic arsenic; CASRN 7440-38-2. U.S. Environmental Protection Agency, Integrated Risk Information System (IRIS) https://iris.epa.gov/ChemicalLanding/&substance_nmbr=278
IRIS. 1995. Chemical Assessment Summary: Mercuric chloride (HgCl2) CASRN 7487-94-7. U.S. Environmental Protection Agency, Integrated Risk Information System (IRIS) https://iris.epa.gov/ChemicalLanding/&substance_nmbr=692
IRIS. 2001. Chemical Assessment Summary: Methylmercury (MeHg); CASRN 22967-92-6. U.S. Environmental Protection Agency, Integrated Risk Information System (IRIS) https://iris.epa.gov/ChemicalLanding/&substance_nmbr=73
Jones, L.M., S.J. Rayson, A.J. Flemming, and P.E. Urwin, 2013. Adaptive and specialised transcriptional responses to xenobiotic stress in Caenorhabditis elegans are regulated by nuclear hormone receptors. PLoS One. 8:e69956. https://doi.org/10.1371/journal.pone.0069956.

Kaletta, T., Hengartner, M.O., 2006. Finding function in novel targets: *C. elegans* as a model organism. Nat Rev Drug Discov. 5, 387–398. https://doi.org/10.1038/nrd2031.

Kang, Y.H., Lee, S.J., 2008. The role of p38 MAPK and JNK in Arsenic trioxide-induced mitochondrial cell death in human cervical cancer cells. J. Cell. Physiol. 217, 23–33. https://doi.org/10.1002/jcp.21470.

Kaplan, R.E.W., Maxwell, C.S., Codd, N.K., Baugh, L.R., 2019. Pervasive Positive and Negative Feedback Regulation of Insulin-Like Signaling in Caenorhabditis elegans. Genetics 211, 349–361. https://doi.org/10.1534/genetics.118.301702.

Kapulkin, W.J., Hiester, B.G., Link, C.D., 2005. Compensatory regulation among ER chaperones in C. elegans. FEBS Lett. 579, 3063–3068. https://doi.org/10.1016/j.febslet.2005.04.062.

Katayama, T., Imaizumi, K., Sato, N., Miyoshi, K., Kudo, T., Hitomi, J., Morihara, T., Yoneda, T., Gomi, F., Mori, Y., Nakano, Y., Takeda, J., Tsuda, T., Itoyama, Y., Murayama, O., Takashima, A., St George-Hyslop, P., Takeda, M., Tohyama, M., 1999. Presenilin-1 mutations downregulate the signalling pathway of the unfolded-protein response. Nat. Cell Biol. 1, 479–485. https://doi.org/10.1038/70265.

Kim, Y., Sun, H., 2007. Functional genomic approach to identify novel genes involved in the regulation of oxidative stress resistance and animal lifespan. Aging Cell 6, 489–503. https://doi.org/10.1111/j.1474-9726.2007.00302.x.

Klosin, A., Casas, E., Hidalgo-Carcedo, C., Vavouri, T., Lehner, B., 2017. Transgenerational transmission of environmental information in *C. elegans*. Science 356, 320–323. https://doi.org/10.1126/science.aah6412.

Kourtis, N., Nikoletopoulou, V., Tavernarakis, N., 2012. Small heat-shock proteins protect from heat-stroke-associated neurodegeneration. Nature 490, 213–218. https://doi.org/10.1038/nature11417.

Kuo, C.T., You, G.T., Jian, Y.J., Chen, T.S., Siao, Y.C., Hsu, A.L., Ching, T.T., 2020. AMPK-mediated formation of stress granules is required for dietary restriction-induced longevity in Caenorhabditis elegans. Aging Cell 19,. https://doi.org/10.1111/acel.13157 e13157.

Lagido, C., D. McLaggan, and L.A. Glover, 2015. A Screenable In Vivo Assay for Mitochondrial Modulators Using Transgenic Bioluminescent Caenorhabditis elegans. J Vis Exp:e53083. https://doi.org/10.3791/53083.

Lau, A., Whitman, S.A., Jaramillo, M.C., Zhang, D.D., 2013. Arsenic-mediated activation of the Nrf2-Keap1 antioxidant pathway. J. Biochem. Mol. Toxicol. 27, 99–105. https://doi.org/10.1002/jbt.21463.

Lee, C., Hong, S., Lee, M.H., Koo, H.-S., Huen, M.-Y., 2015. A PHF8 Homolog in C. elegans Promotes DNA Repair via Homologous Recombination. PLoS ONE 10 (4), e0123865.

Leiers, B., Kampkotter, A., Grevelding, C.G., Link, C.D., Johnson, T.E., Henkle-Duhrsen, K., 2003. A stress-responsive glutathione S-transferase confers resistance to oxidative stress in Caenorhabditis elegans. Free Radic Biol Med. 34, 1405–1415. https://doi.org/10.1016/s0891-5849(03)00102-3.

Leung, M.C., Williams, P.L., Benedetto, A., Au, C., Helmcke, K.J., Aschner, M., Meyer, J. N., 2008. *Caenorhabditis elegans*: an emerging model in biomedical and environmental toxicology. Toxicol. Sci. 106, 5–28. https://doi.org/10.1093/toxsci/kfn121.

Lezzerini, M., Budovskaya, Y., 2014. A dual role of the Wnt signaling pathway during aging in Caenorhabditis elegans. Aging Cell 13, 8–18. https://doi.org/10.1111/acel.12141.

Li, Y., Gao, S., Jing, H., Qi, L., Ning, J., Tan, Z., Yang, K., Zhao, C., Ma, L., Li, G., 2013. Correlation of chemical acute toxicity between the nematode and the rodent. Toxicol. Res. 2, 403–412. https://doi.org/10.1039/c3tx50039j.

Limjindaporn, T., Wongwiwat, W., Noisakran, S., Srisawat, C., Netsawang, J., Puttikhunt, C., Kasinrerk, W., Avirutnan, P., Thiemmeca, S., Sriburi, R., Sittisombut, N., Malasit, P., Yenchitsomanus, P.T., 2009. Interaction of dengue virus envelope protein with endoplasmic reticulum-resident chaperones facilitates dengue virus production. Biochem. Biophys. Res. Commun. 379, 196–200. https://doi.org/10.1016/j.bbrc.2008.12.070.

Luvonga, C., Rimmer, C.A., Yu, L.L., Lee, S.B., 2020. Analytical Methodologies for the Determination of Organoarsenicals in Edible Marine Species: A Review. J. Agric. Food Chem. 68, 1910–1934. https://doi.org/10.1021/acs.jafc.9b04525.

Luz, A.L., Godebo, T.R., Bhatt, D.P., Ilkayeva, O.R., Maurer, L.L., Hirschey, M.D., Meyer, J.N., 2016. From the Cover: Arsenite Uncouples Mitochondrial Respiration and Induces a Warburg-like Effect in Caenorhabditis elegans. Toxicol. Sci. 152, 349–362. https://doi.org/10.1093/toxsci/kfw093.

Luz, A.L., Godebo, T.R., Smith, L.L., Leuthner, T.C., Maurer, L.L., Meyer, J.N., 2017. Deficiencies in mitochondrial dynamics sensitize Caenorhabditis elegans to arsenite and other mitochondrial toxicants by reducing mitochondrial adaptability. Toxicology 387, 81–94. https://doi.org/10.1016/j.tox.2017.05.018.

Ma, W., Yue, J., Liang, S., Gao, M., Wang, X., Cui, N., Li, H., Zhi, D., 2021. Realgar increases defenses against infection by Enterococcus faecalis in Caenorhabditis elegans. J. Ethnopharmacol. 268,. https://doi.org/10.1016/j.jep.2020.113559 113559.

Marsh, D.O., Clarkson, T.W., Myers, G.J., Davidson, P.W., Cox, C., Cernichiari, E., Tanner, M.A., Lednar, W., Shamlaye, C., Choisy, O., et al, 1995. The Seychelles study of fetal methylmercury exposure and child development: introduction. Neurotoxicology. 16, 583–596.

Martinez-Finley, E.J., Caito, S., Slaughter, J.C., Aschner, M., 2013a. The Role of skn-1 in methylmercury-induced latent dopaminergic neurodegeneration. Neurochem. Res. 38, 2650–2660. https://doi.org/10.1007/s11064-013-1183-0.

Martinez-Finley, E.J., Chakraborty, S., Slaughter, J.C., Aschner, M., 2013b. Early-life exposure to methylmercury in wildtype and pdr-1/parkin knockout *C. elegans*. Neurochem. Res. 38, 1543–1552. https://doi.org/10.1007/s11064-013-1054-8.

Masjosthusmann, S., Barenys, M., El-Gamal, M., Geerts, L., Gerosa, L., Gorreja, A., Kühne, B., Marchetti, N., Tigges, J., Viviani, B., Witters, H., Fritsche, E., 2018. Literature review and appraisal on alternative neurotoxicity testing methods. EFS3 15 (4).

Matilainen, O., Ribeiro, A.R.S., Verbeeren, J., Cetinbas, M., Sadreyev, R.I., Garcia, S.M. D.A., 2021. Loss of Muscleblind Splicing Factor Shortens C. elegans Lifespan by Reducing the Activity of p38 MAPK/PMK-1 and Transcription Factors ATF-7 and Nrf/SKN-1. BioRxiv Cold Spring Harbor Laboratory.

McElwee, J., Bubb, K., Thomas, J.H., 2003. Transcriptional outputs of the Caenorhabditis elegans forkhead protein DAF-16. Aging Cell 2 (2), 111–121.

McElwee, M.K., Freedman, J.H., 2011. Comparative toxicology of mercurials in Caenorhabditis elegans. Environ. Toxicol. Chem. 30, 2135–2141. https://doi.org/10.1002/etc.603.

McElwee, M.K., Ho, L.A., Chou, J.W., Smith, M.V., Freedman, J.H., 2013. Comparative toxicogenomic responses of mercuric and methyl-mercury. BMC Genomics 14, 698. https://doi.org/10.1186/1471-2164-14-698.

Mikoláš, P., J. Kollárová, K. Šebková, V. Saudek, P. Yilma, M. Kostrouchová, M.W. Krause, Z. Kostrouch, and M. Kostrouchová, 2013. GEI-8, a Homologue of Vertebrate Nuclear Receptor Corepressor NCoR/SMRT, Regulates Gonad Development and Neuronal Functions in Caenorhabditis elegans. PLOS ONE. 8: e58462. https://doi.org/10.1371/journal.pone.0058462.

Miller, D.L., M.W. Budde, and M.B. Roth, 2011. HIF-1 and SKN-1 coordinate the transcriptional response to hydrogen sulfide in Caenorhabditis elegans. PLoS One. 6: e25476. https://doi.org/10.1371/journal.pone.0025476.

Minniti, A.N., Cataldo, R., Trigo, C., Vasquez, L., Mujica, P., Leighton, F., Inestrosa, N.C., Aldunate, R., 2009. Methionine sulfoxide reductase A expression is regulated by the DAF-16/FOXO pathway in Caenorhabditis elegans. Aging Cell 8, 690–705. https://doi.org/10.1111/j.1474-9726.2009.00521.x.

Muir, R.E., Tan, M.W., 2008. Virulence of Leucobacter chromiireducens subsp. solipictus to Caenorhabditis elegans: characterization of a novel host-pathogen interaction. Appl. Environ. Microbiol. 74, 4185–4198. https://doi.org/10.1128/AEM.00381-08.

Mullenix, P.J., 1989. Evolution of motor activity tests into a screening reality. Toxicol. Ind. Health 5, 203–219. https://doi.org/10.1177/074823378900500206.

Murphy, C.T., McCarroll, S.A., Bargmann, C.I., Fraser, A., Kamath, R.S., Ahringer, J., Li, H., Kenyon, C., 2003. Genes that act downstream of DAF-16 to influence the lifespan of Caenorhabditis elegans. Nature 424, 277–283. https://doi.org/10.1038/nature01789.

Myers, G.J., Davidson, P.W., Cox, C., Shamlaye, C.F., Tanner, M.A., Choisy, O., Sloane-Reeves, J., Marsh, D., Cernichiari, E., Choi, A., et al, 1995. Neurodevelopmental outcomes of Seychellois children sixty-six months after in utero exposure to methylmercury from a maternal fish diet: pilot study. Neurotoxicology. 16, 639–652.

Naess, S., Aakre, I., Lundebye, A.K., Ornsrud, R., Kjellevold, M., Markhus, M.W., Dahl, L., 2020. Mercury, lead, arsenic, and cadmium in Norwegian seafood products and consumer exposure. Food Addit Contam Part B Surveill. 13, 99–106. https://doi.org/10.1080/19393210.2020.1735533.

Nag, P., Aggarwal, P.R., Ghosh, S., Narula, K., Tayal, R., Maheshwari, N., Chakraborty, N., Chakraborty, S., 2017. Interplay of neuronal and non-neuronal genes regulates intestinal DAF-16-mediated immune response during Fusarium infection of Caenorhabditis elegans. Cell Death Discov. 3, 17073. https://doi.org/10.1038/cddiscovery.2017.73.

Naidoo, N., Zhu, J., Galante, R.J., Lian, J., Strus, E., Lee, A., Keenan, B.T., Pack, A.I., 2018. Reduction of the molecular chaperone binding immunoglobulin protein (BiP) accentuates the effect of aging on sleep-wake behavior. Neurobiol. Aging 69, 10–25. https://doi.org/10.1016/j.neurobiolaging.2018.04.011.

Narbonne, P., Roy, R., 2009. Caenorhabditis elegans dauers need LKB1/AMPK to ration lipid reserves and ensure long-term survival. Nature 457, 210–214. https://doi.org/10.1038/nature07536.

Nass, R., Hamza, I., 2007. The nematode C. elegans as an animal model to explore toxicology in vivo: solid and axenic growth culture conditions and compound exposure parameters. Curr Protoc Toxicol. Chapter 1 (Unit1), 9. https://doi.org/10.1002/0471140856.tx0109s31.

O'Rourke, D., Baban, D., Demidova, M., Mott, R., Hodgkin, J., 2006. Genomic clusters, putative pathogen recognition molecules, and antimicrobial genes are induced by infection of C. elegans with M. nematophilum. Genome Res. 16, 1005–1016. https://doi.org/10.1101/gr.50823006.

Oh, S.W., Mukhopadhyay, A., Dixit, B.L., Raha, T., Green, M.R., Tissenbaum, H.A., 2006. Identification of direct DAF-16 targets controlling longevity, metabolism and diapause by chromatin immunoprecipitation. Nat. Genet. 38, 251–257. https://doi.org/10.1038/ng1723.

Oliveira, R.P., Porter Abate, J., Dilks, K., Landis, J., Ashraf, J., Murphy, C.T., Blackwell, T.K., 2009. Condition-adapted stress and longevity gene regulation by Caenorhabditis elegans SKN-1/Nrf. Aging Cell 8, 524–541. https://doi.org/10.1111/j.1474-9726.2009.00501.x.

Paek, J., Lo, J.Y., Narasimhan, S.D., Nguyen, T.N., Glover-Cutter, K., Robida-Stubbs, S., Suzuki, T., Yamamoto, M., Blackwell, T.K., Curran, S.P., 2012. Mitochondrial SKN-1/Nrf mediates a conserved starvation response. Cell Metab. 16, 526–537. https://doi.org/10.1016/j.cmet.2012.09.007.

Parish, S.T., Aschner, M., Casey, W., Corvaro, M., Embry, M.R., Fitzpatrick, S., Kidd, D., Kleinstreuer, N.C., Lima, B.S., Settivari, R.S., Wolf, D.C., Yamazaki, D., Boobis, A., 2020. An evaluation framework for new approach methodologies (NAMs) for human health safety assessment. Regul. Toxicol. Pharm. 112,. https://doi.org/10.1016/j.yrtph.2020.104592 104592.

Park, S.K., Tedesco, P.M., Johnson, T.E., 2009. Oxidative stress and longevity in Caenorhabditis elegans as mediated by SKN-1. Aging Cell 8, 258–269. https://doi.org/10.1111/j.1474-9726.2009.00473.x.

Prince, L.M., Rand, M.D., 2018. Methylmercury exposure causes a persistent inhibition of myogenin expression and C2C12 myoblast differentiation. Toxicology 393, 113–122. https://doi.org/10.1016/j.tox.2017.11.002.

Przybysz, A.J., Choe, K.P., Roberts, L.J., Strange, K., 2009. Increased age reduces DAF-16 and SKN-1 signaling and the hormetic response of Caenorhabditis elegans to the xenobiotic juglone. Mech. Ageing Dev. 130, 357–369. https://doi.org/10.1016/j.mad.2009.02.004.

Pujol, N., Zugasti, O., Wong, D., Couillault, C., Kurz, C.L., Schulenburg, H., Ewbank, J.J., Ausubel, F.M., 2008. Anti-fungal innate immunity in *C. elegans* is enhanced by evolutionary diversification of antimicrobial peptides. PLoS Pathog. 4 (7), e1000105.

Pukkila-Worley, R., F.M. Ausubel, and E. Mylonakis, 2011. Candida albicans infection of Caenorhabditis elegans induces antifungal immune defenses. PLoS Pathog. 7: e1002074. https://doi.org/10.1371/journal.ppat.1002074.

Rains, M.E., Muncie, C.B., Pang, Y.i., Fan, L.-W., Tien, L.-T., Ojeda, N.B., 2021. Oxidative Stress and Neurodevelopmental Outcomes in Rat Offspring with Intrauterine Growth Restriction Induced by Reduced Uterine Perfusion. Brain Sci. 11 (1), 78.

Ren, M., Feng, H., Fu, Y., Land, M., Rubin, C.S., 2009. Protein kinase D is an essential regulator of C. elegans innate immunity. Immunity 30, 521–532. https://doi.org/10.1016/j.immuni.2009.03.007.

Ruszkiewicz, J.A., Pinkas, A., Miah, M.R., Weitz, R.L., Lawes, M.J.A., Akinyemi, A.J., Ijomone, O.M., Aschner, M., 2018. *C. elegans* as a model in developmental neurotoxicology. Toxicol. Appl. Pharmacol. 354, 126–135.

Sahu, S.N., J. Lewis, I. Patel, S. Bozdag, J.H. Lee, R. Sprando, and H.N. Cinar, 2013. Genomic analysis of stress response against arsenic in Caenorhabditis elegans. PLoS One. 8:e66431. https://doi.org/10.1371/journal.pone.0066431.

Schalock, R.L., Brown, W.J., Kark, R.A., Menon, N.K., 1981. Perinatal methylmercury intoxication: behavioral effects in rats. Dev. Psychobiol. 14, 213–219. https://doi.org/10.1002/dev.420140310.

Schifano, E., Ficociello, G., Vespa, S., Ghosh, S., Cipollo, J.F., Talora, C., Lotti, L.V., Mancini, P., Uccelletti, D., 2019. Pmr-1 gene affects susceptibility of Caenorhabditis elegans to Staphylococcus aureus infection through glycosylation and stress response pathways' alterations. Virulence. 10, 1013–1025. https://doi.org/10.1080/21505594.2019.1697118.

Schlebusch, C.M., Gattepaille, L.M., Engstrom, K., Vahter, M., Jakobsson, M., Broberg, K., 2015. Human adaptation to arsenic-rich environments. Mol. Biol. Evol. 32, 1544–1555. https://doi.org/10.1093/molbev/msv046.

Settivari, R., VanDuyn, N., LeVora, J., Nass, R., 2013. The Nrf2/SKN-1-dependent glutathione S-transferase pi homologue GST-1 inhibits dopamine neuron degeneration in a Caenorhabditis elegans model of manganism. Neurotoxicology. 38, 51–60. https://doi.org/10.1016/j.neuro.2013.05.014.

Seydoux, G., Savage, C., Greenwald, I., 1993. Isolation and characterization of mutations causing abnormal eversion of the vulva in Caenorhabditis elegans. Dev. Biol. 157, 423–436. https://doi.org/10.1006/dbio.1993.1146.

Shin, H., Lee, H., Fejes, A.P., Baillie, D.L., Koo, H.S., Jones, S.J., 2011. Gene expression profiling of oxidative stress response of *C. elegans* aging defective AMPK mutants using massively parallel transcriptome sequencing. BMC Res Notes. 4 (34). https://doi.org/10.1186/1756-0500-4-34.

Simonetta, S.H., 2010. Towards an automatic method for toxicity and pharmacological testing in *C. elegans*. The Worm Breeder's. Gazette. 18 (10).

Sok, J., Calfon, M., Lu, J., Lichtlen, P., Clark, S.G., Ron, D., 2001. Arsenite-inducible RNA-associated protein (AIRAP) protects cells from arsenite toxicity. Cell Stress Chaperones. 6, 6–15. https://doi.org/10.1379/1466-1268(2001)006<0006:airapa>2.0.co;2.

Sprando, R.L., Olejnik, N., Cinar, H.N., Ferguson, M., 2009. A method to rank order water soluble compounds according to their toxicity using *Caenorhabditis elegans*, a Complex Object Parametric Analyzer and Sorter, and axenic liquid media. Food Chem. Toxicol. 47, 722–728. https://doi.org/10.1016/j.fct.2009.01.007.

Stanhill, A., Haynes, C.M., Zhang, Y., Min, G., Steele, M.C., Kalinina, J., Martinez, E., Pickart, C.M., Kong, X.P., Ron, D., 2006. An arsenite-inducible 19S regulatory particle-associated protein adapts proteasomes to proteotoxicity. Mol. Cell 23, 875–885. https://doi.org/10.1016/j.molcel.2006.07.023.

Steinbaugh, M.J., Narasimhan, S.D., Robida-Stubbs, S., Moronetti Mazzeo, L.E., Dreyfuss, J.M., Hourihan, J.M., Raghavan, P., Operana, T.N., Esmaillie, R., Blackwell, T.K., 2015. Lipid-mediated regulation of SKN-1/Nrf in response to germ cell absence. Elife. 4. https://doi.org/10.7554/eLife.07836.

Tam, L.M., Wang, Y., 2020. Arsenic Exposure and Compromised Protein Quality Control. Chem. Res. Toxicol. 33, 1594–1604. https://doi.org/10.1021/acs.chemrestox.0c00107.

Tan, L., Wang, S., Wang, Y., He, M., Liu, D., 2015. Bisphenol A exposure accelerated the aging process in the nematode Caenorhabditis elegans. Toxicol. Lett. 235, 75–83. https://doi.org/10.1016/j.toxlet.2015.03.010.

Taylor, R.C., Dillin, A., 2013. XBP-1 Is a Cell-Nonautonomous Regulator of Stress Resistance and Longevity. Cell 153, 1435–1447 https://doi.org/10.1016/j.cell.2013.05.042.

Teixeira, F.B., de Oliveira, A.C.A., Leao, L.K.R., Fagundes, N.C.F., Fernandes, R.M., Fernandes, L.M.P., da Silva, M.C.F., Amado, L.L., Sagica, F.E.S., de Oliveira, E.H.C., Crespo-Lopez, M.E., Maia, C.S.F., Lima, R.R., 2018. Exposure to Inorganic Mercury Causes Oxidative Stress, Cell Death, and Functional Deficits in the Motor Cortex. Front. Mol. Neurosci. 11, 125. https://doi.org/10.3389/fnmol.2018.00125.

Tepper, R.G., Ashraf, J., Kaletsky, R., Kleemann, G., Murphy, C.T., Bussemaker, H.J., 2013. PQM-1 complements DAF-16 as a key transcriptional regulator of DAF-2-mediated development and longevity. Cell 154, 676–690. https://doi.org/10.1016/j.cell.2013.07.006.

Thomas, D.J., Styblo, M., Lin, S., 2001. The cellular metabolism and systemic toxicity of arsenic. Toxicol. Appl. Pharmacol. 176, 127–144. https://doi.org/10.1006/taap.2001.9258.

Tian, Y., Garcia, G., Bian, Q., Steffen, K.K., Joe, L., Wolff, S., Meyer, B.J., Dillin, A., 2016. Mitochondrial Stress Induces Chromatin Reorganization to Promote Longevity and UPR(mt). Cell 165, 1197–1208. https://doi.org/10.1016/j.cell.2016.04.011.

Torres-Cuevas, I., Parra-Llorca, A., Sanchez-Illana, A., Nunez-Ramiro, A., Kuligowski, J., Chafer-Pericas, C., Cernada, M., Escobar, J., Vento, M., 2017. Oxygen and oxidative stress in the perinatal period. Redox Biol. 12, 674–681. https://doi.org/10.1016/j.redox.2017.03.011.

Toyama, T., Sumi, D., Shinkai, Y., Yasutake, A., Taguchi, K., Tong, K.I., Yamamoto, M., Kumagai, Y., 2007. Cytoprotective role of Nrf2/Keap1 system in methylmercury toxicity. Biochem. Biophys. Res. Commun. 363, 645–650. https://doi.org/10.1016/j.bbrc.2007.09.017.

Troemel, E.R., Chu, S.W., Reinke, V., Lee, S.S., Ausubel, F.M., Kim, D.H., 2006. p38 MAPK regulates expression of immune response genes and contributes to longevity in *C. elegans*. PLoS Genet. 2 (11), e183.

Tsialikas, J., and Y. Argon, 2017. xbp-1 mRNA splicing is attenuated under prolonged exposure to ER stress. MicroPubl Biol. 2017. https://doi.org/10.17912/W2707X.

Tucker, E.K., Nowak, R.A., 2018. Methylmercury alters proliferation, migration, and antioxidant capacity in human HTR8/SV-neo trophoblast cells. Reprod. Toxicol. 78, 60–68. https://doi.org/10.1016/j.reprotox.2018.03.008.

Tullet, J.M., Hertweck, M., An, J.H., Baker, J., Hwang, J.Y., Liu, S., Oliveira, R.P., Baumeister, R., Blackwell, T.K., 2008. Direct inhibition of the longevity-promoting factor SKN-1 by insulin-like signaling in C. elegans. Cell 132, 1025–1038. https://doi.org/10.1016/j.cell.2008.01.030.

Twaddle, N.C., Vanlandingham, M., Beland, F.A., Doerge, D.R., 2018. Metabolism and disposition of arsenic species after repeated oral dosing with sodium arsenite in drinking water. II. Measurements in pregnant and fetal CD-1 mice. Food Chem. Toxicol. 115, 178–184. https://doi.org/10.1016/j.fct.2018.03.010.

VanDuyn, N., Settivari, R., Wong, G., Nass, R., 2010. SKN-1/Nrf2 inhibits dopamine neuron degeneration in a *Caenorhabditis elegans* model of methylmercury toxicity. Toxicol. Sci. 118, 613–624. https://doi.org/10.1093/toxsci/kfq285.

Wan, J., Yuan, L., Jing, H., Zheng, Q., Xiao, H., 2021. Defective apoptotic cell clearance activates innate immune response to protect Caenorhabditis elegans against pathogenic bacteria. Virulence. 12, 75–83. https://doi.org/10.1080/21505594.2020.1857982.

Wang, F., Liu, S., Xi, S., Yan, L., Wang, H., Song, Y., Sun, G., 2013. Arsenic induces the expressions of angiogenesis-related factors through PI3K and MAPK pathways in SV-HUC-1 human uroepithelial cells. Toxicol. Lett. 222, 303–311. https://doi.org/10.1016/j.toxlet.2013.08.008.

Wang, J., Robida-Stubbs, S., Tullet, J.M.A., Rual, J.-F., Vidal, M., Blackwell, T.K., Kim, S.K., 2010. RNAi screening implicates a SKN-1-dependent transcriptional response in stress resistance and longevity deriving from translation inhibition. PLoS Genet. 6 (8), e1001048.

Watanabe, N., Morimatsu, M., Fujita, A., Teranishi, M., Sudevan, S., Watanabe, M., Iwasa, H., Hata, Y., Kagi, H., Nishiyama, M., Naruse, K., Higashitani, A., 2020. Increased hydrostatic pressure induces nuclear translocation of DAF-16/FOXO in *C. elegans*. Biochem. Biophys. Res. Commun. 523, 853–858. https://doi.org/10.1016/j.bbrc.2020.01.047.

WHO. 1991. Inorganic mercury. United Nations Environment Programme http://www.inchem.org/documents/ehc/ehc/ehc118.htm

Wong, D., Bazopoulou, D., Pujol, N., Tavernarakis, N., Ewbank, J.J., 2007. Genome-wide investigation reveals pathogen-specific and shared signatures in the response of *Caenorhabditis elegans* to infection. Genome Biol. 8, R194. https://doi.org/10.1186/gb-2007-8-9-r194.

WormBase. 2021. SimpleMine. https://wormbase.org//tools/mine/simplemine.cgi.

Wyatt, L.H., Diringer, S.E., Rogers, L.A., Hsu-Kim, H., Pan, W.K., Meyer, J.N., 2016. Antagonistic Growth Effects of Mercury and Selenium in Caenorhabditis elegans Are Chemical-Species-Dependent and Do Not Depend on Internal Hg/Se Ratios. Environ. Sci. Technol. 50, 3256–3264. https://doi.org/10.1021/acs.est.5b06044.

Wyatt, L.H., Luz, A.L., Cao, X., Maurer, L.L., Blawas, A.M., Aballay, A., Pan, W.K., Meyer, J.N., 2017. Effects of methyl and inorganic mercury exposure on genome homeostasis and mitochondrial function in Caenorhabditis elegans. DNA Repair (Amst). 52, 31–48. https://doi.org/10.1016/j.dnarep.2017.02.005.

Yamagishi, N., Ueda, T., Mori, A., Saito, Y., Hatayama, T., 2012. Decreased expression of endoplasmic reticulum chaperone GRP78 in liver of diabetic mice. Biochem. Biophys. Res. Commun. 417, 364–370. https://doi.org/10.1016/j.bbrc.2011.11.118.

Yanase, S., Yasuda, K., Ishii, N., 2020. Interaction between the ins/IGF-1 and p38 MAPK signaling pathways in molecular compensation of sod genes and modulation related to intracellular ROS levels in C. elegans. Biochem. Biophys. Rep. 23 (100796). https://doi.org/10.1016/j.bbrep.2020.100796.

Yang, C., Frenkel, K., 2002. Arsenic-mediated cellular signal transduction, transcription factor activation, and aberrant gene expression: implications in carcinogenesis. J. Environ. Pathol. Toxicol. Oncol. 21, 331–342.

Yang, W., Dierking, K., Rosenstiel, P.C., Schulenburg, H., 2016. GATA transcription factor as a likely key regulator of the Caenorhabditis elegans innate immune response against gut pathogens. Zoology (Jena). 119, 244–253. https://doi.org/10.1016/j.zool.2016.05.013.

Yu, C.W., How, C.M., Liao, V.H., 2016. Arsenite exposure accelerates aging process regulated by the transcription factor DAF-16/FOXO in Caenorhabditis elegans. Chemosphere 150, 632–638. https://doi.org/10.1016/j.chemosphere.2016.01.004.

Zárate-Potes, A., Yang, W., Pees, B., Schalkowski, R., Segler, P., Andresen, B., Haase, D., Nakad, R., Rosenstiel, P., Tetreau, G., Colletier, J.-P., Schulenburg, H., Dierking, K., Collins, J.J., 2020. The C. elegans GATA transcription factor elt-2 mediates distinct transcriptional responses and opposite infection outcomes towards different Bacillus thuringiensis strains. PLoS Pathog. 16 (9), e1008826.

Zdraljevic, S., Fox, B.W., Strand, C., Panda, O., Tenjo, F.J., Brady, S.C., Crombie, T.A., Doench, J.G., Schroeder, F.C., Andersen, E.C., 2019. Natural variation in C. elegans arsenic toxicity is explained by differences in branched chain amino acid metabolism. Elife. 8. https://doi.org/10.7554/eLife.40260.